Understanding localised corrosion phenomena by using the synergies of thermodynamics and diffusion

Michael Auinger

July, 3rd 2014

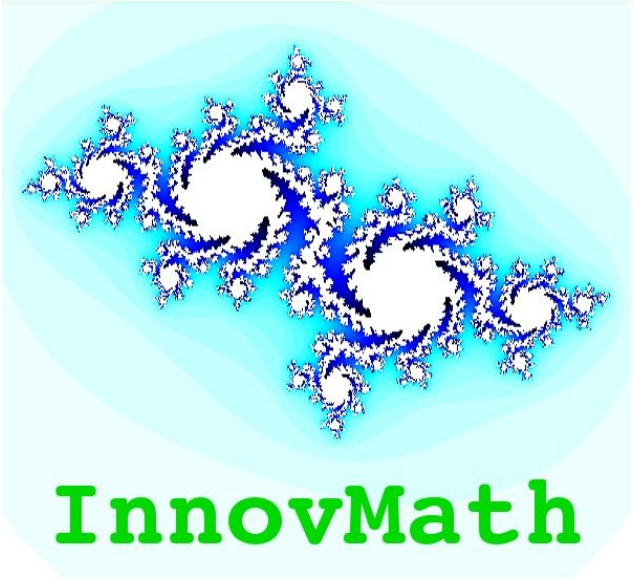

Presentation at: GTT Users Meeting 2014
Herzogenrath (Aachen, Germany)

Outlook

- Introduction
  - Finding Localised Corrosion Phenomena
  - Modelling Approach
- Examples
  - Decarbursation of Pearlite
  - High Temperature Corrosion
  - Hydrogen in Steels
  - Electrochemical Corrosion
- Summary

Industrial Hot-Rolling Process

InnovMath

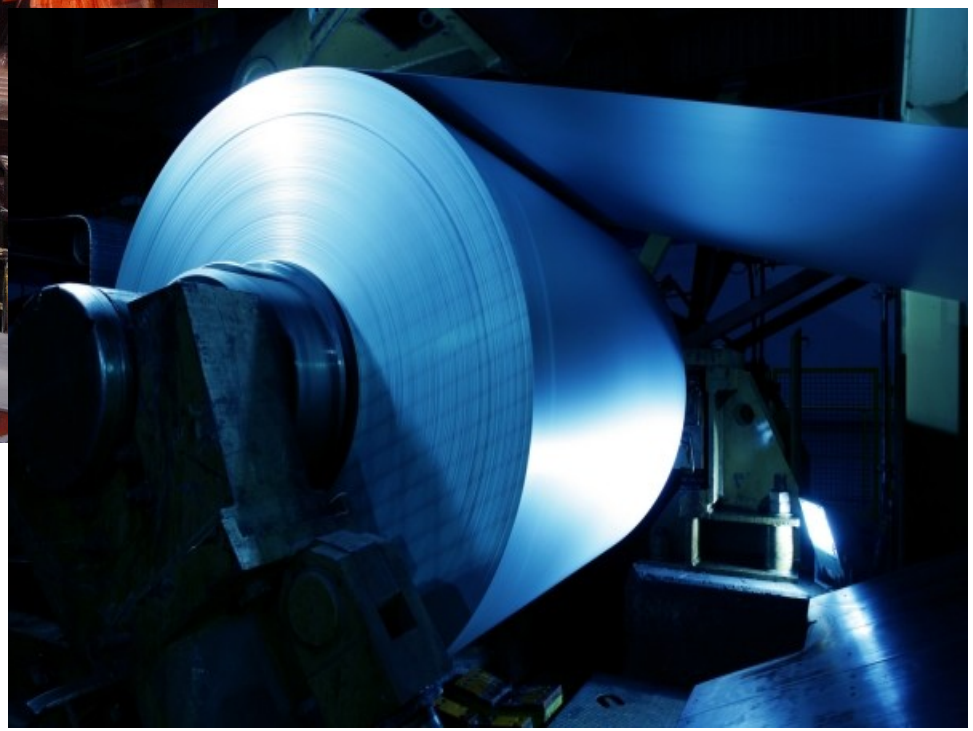

(Internal) Oxidation Scheme

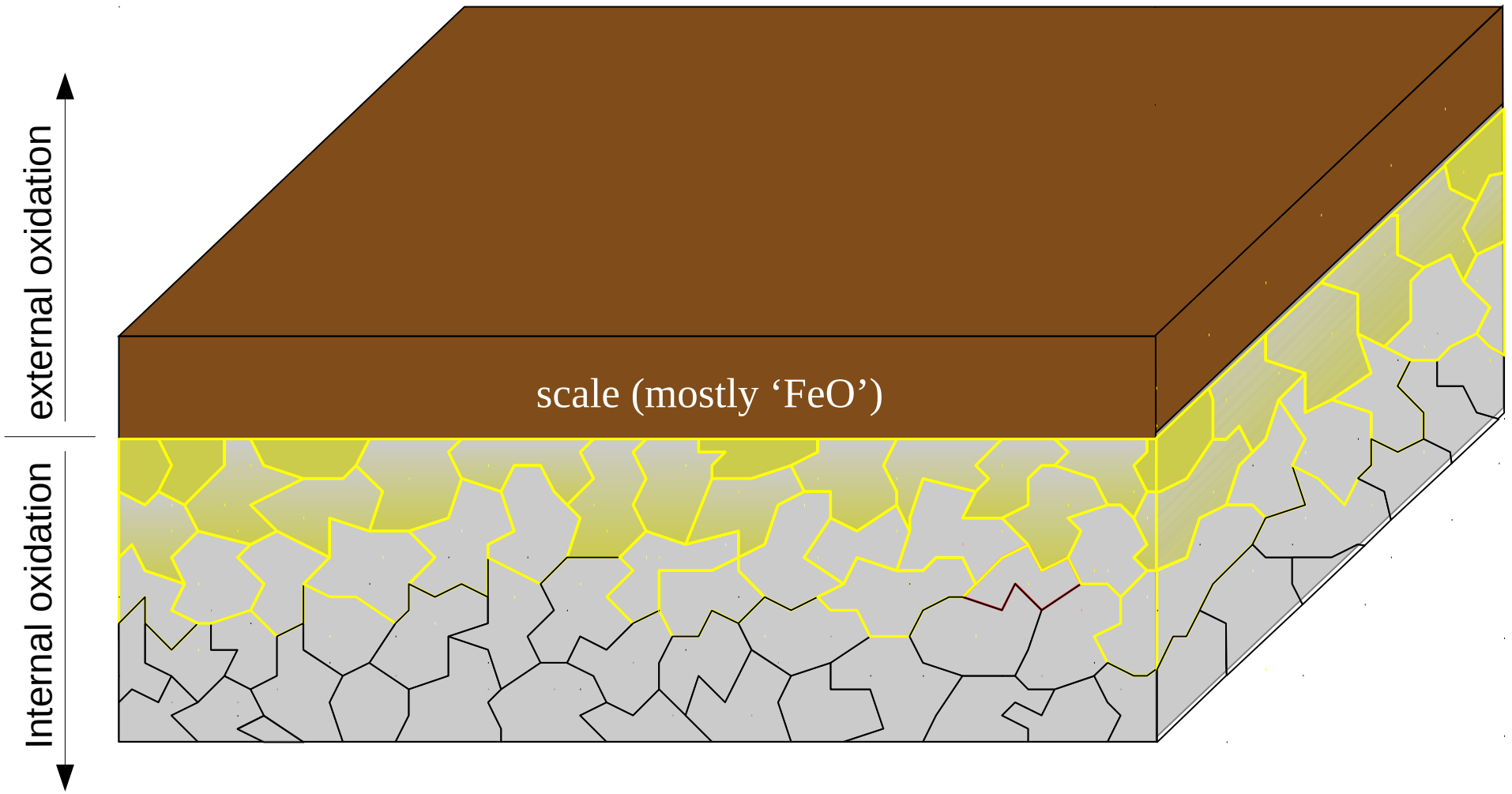

Ellingham-Diagram

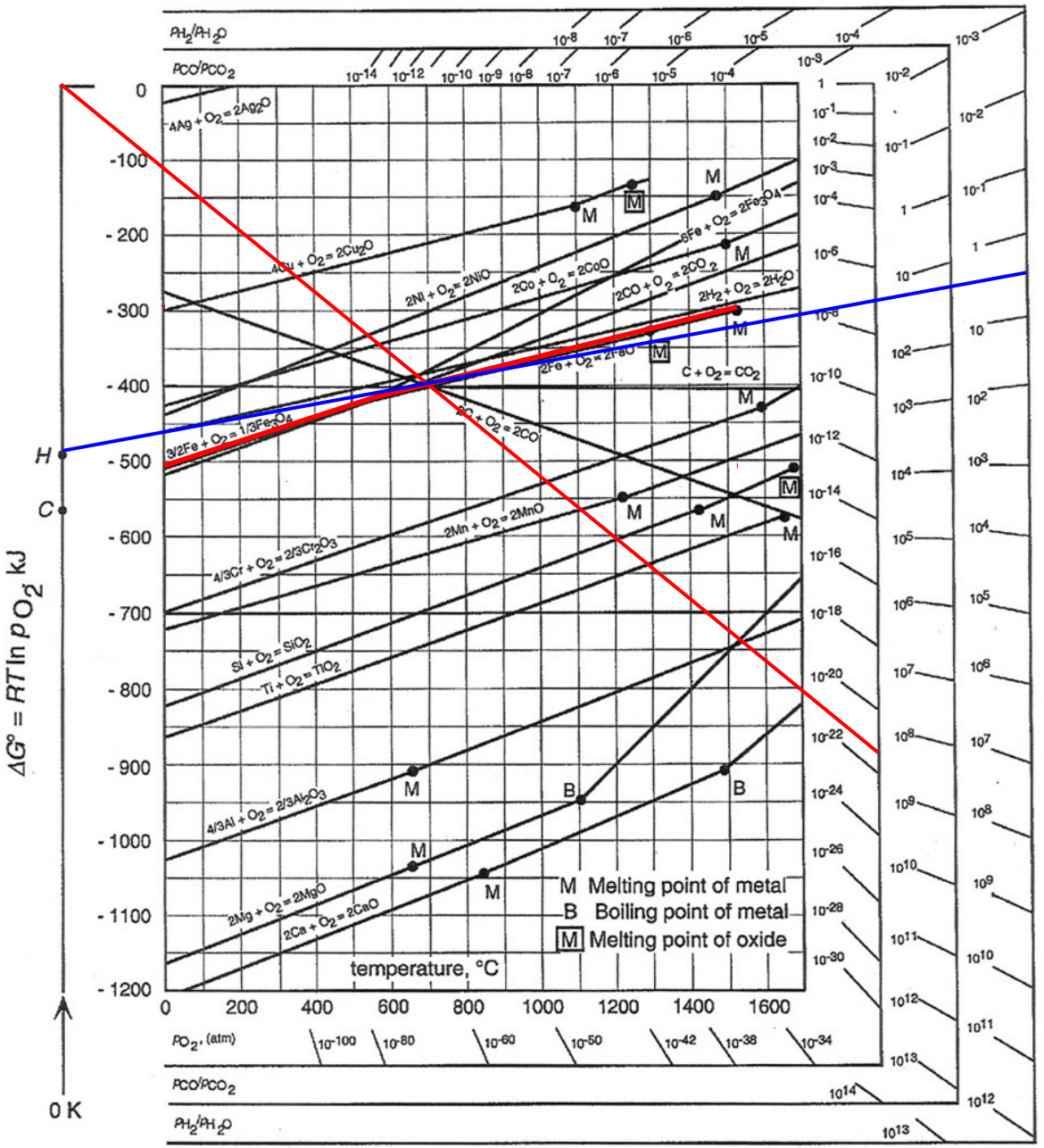

History of Diffusion

~1600 Japan: Mokume-Gane (木目金)

Combination of two (or more) metals by “diffusion welding”

Knife and Sword

Rings and Jewellery

www.wikipedia.org (dl 12.10.2010)

(Recent) History of Diffusion

From the latin word *diffundere* = disperse, spread

1833 *Thomas Graham*
first observations and hypotheses

1855 *Adolf Fick*
first empirical formulas

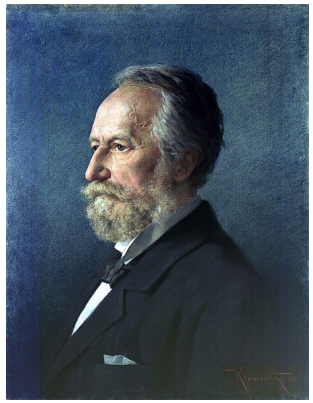

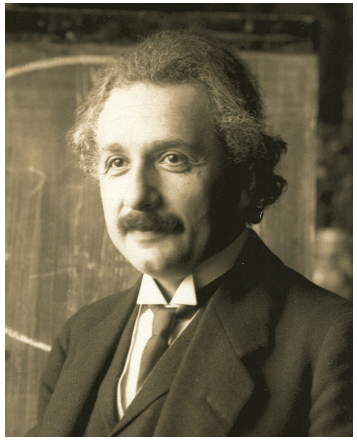

1905 *Albert Einstein,*
1906 *Marian Smoluchowski*
generalized theory

$$D \propto \frac{X^2}{t}$$

Program Structure

element transport ⇄ chemical reaction

$$\frac{dc_{i(x,t)}}{dt} = \mathrm{div}\left(D_{i(x,T)}.\nabla c_{i(x,t)}\right)$$

CHEMAPP

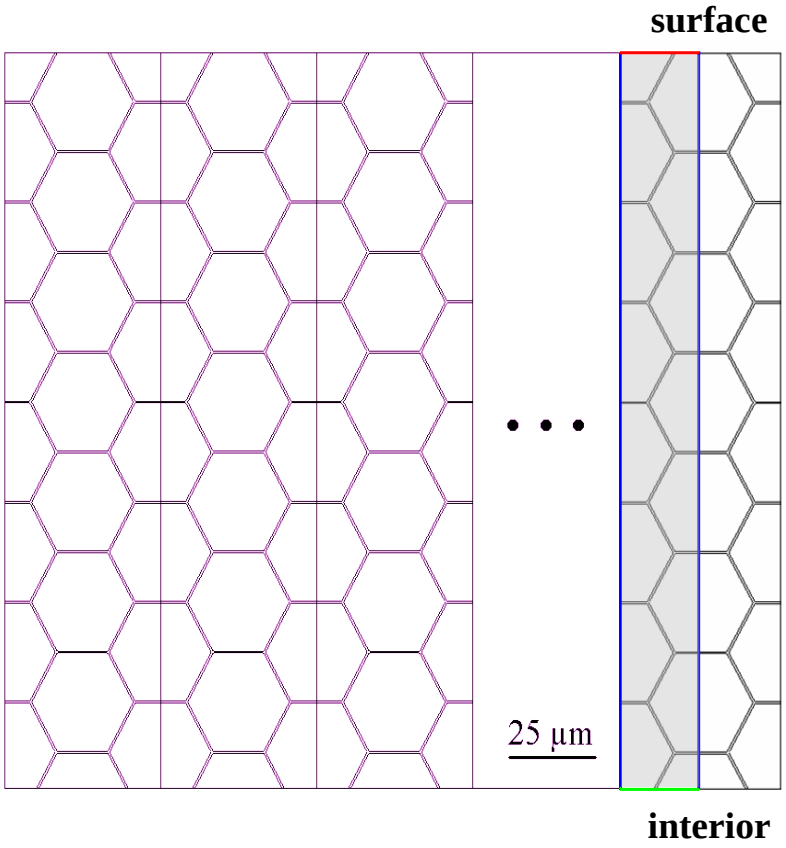

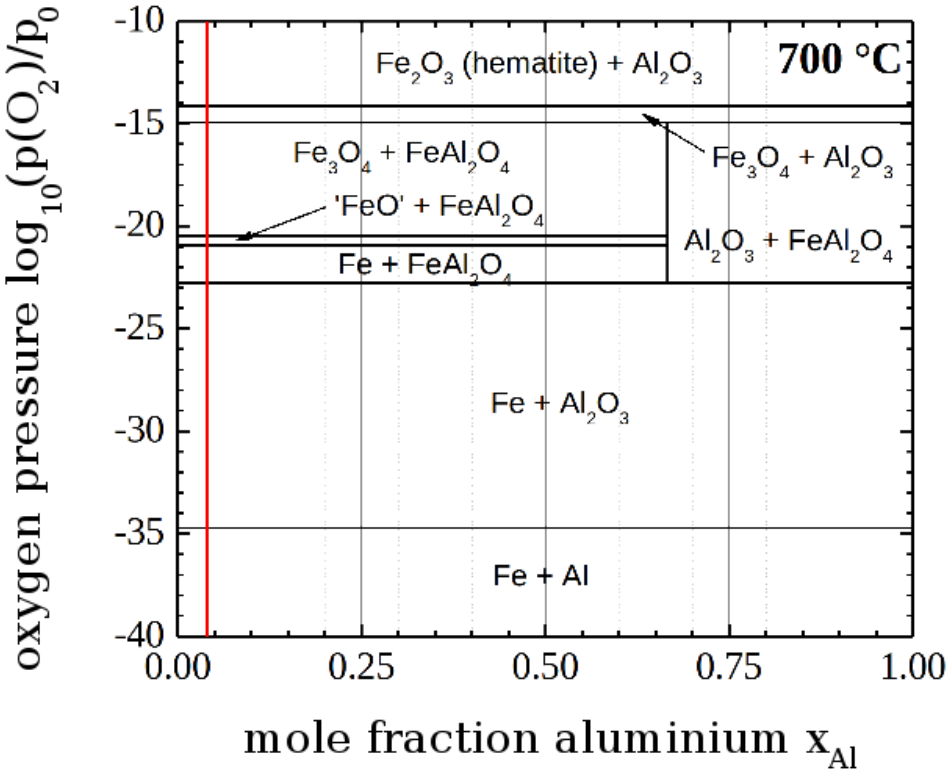

"ASTRID", Oxid. Met.. **76** (2011) 247-258.

Program Output (Fe-Mn-Cr alloy)

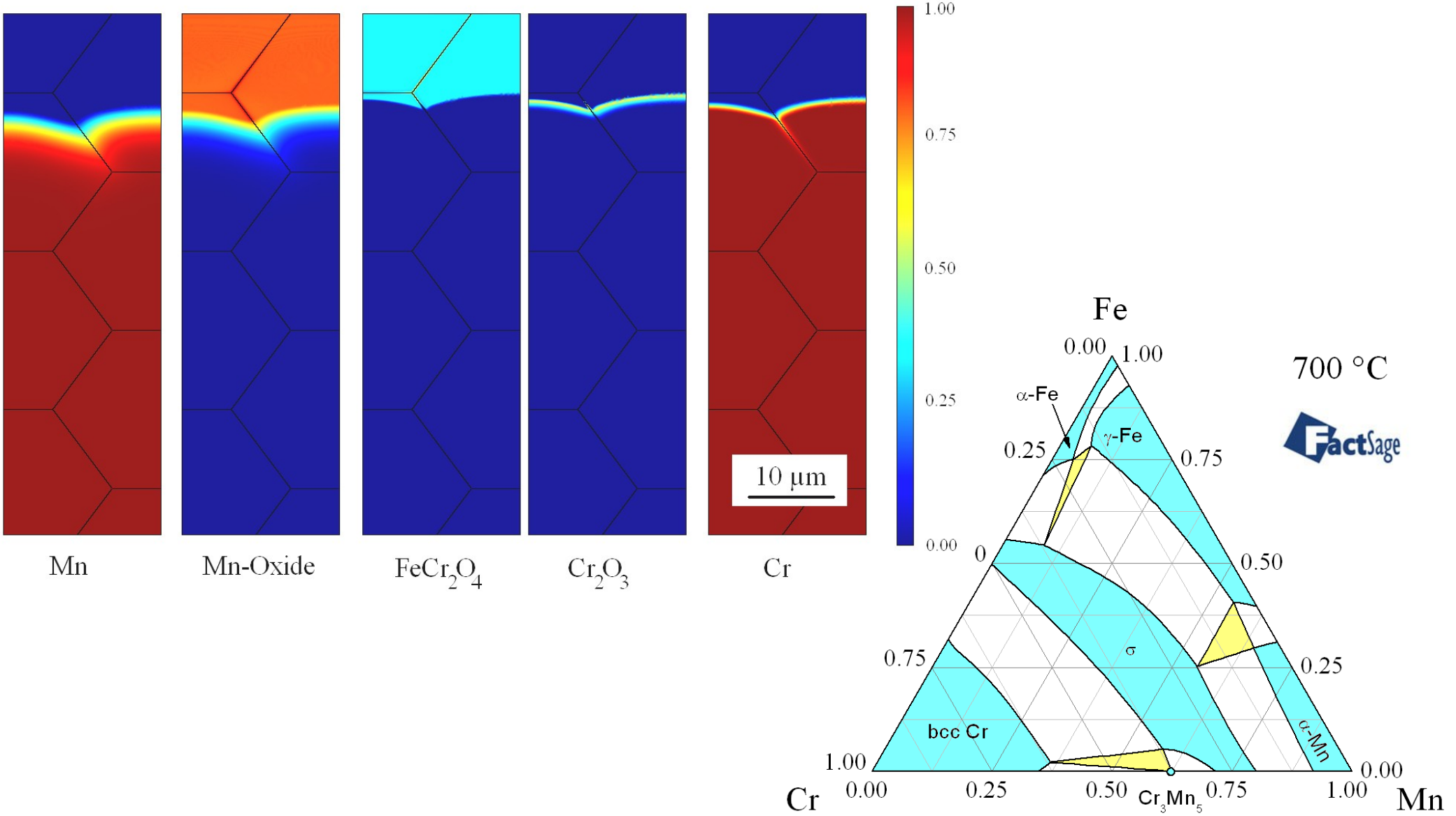

Figure: Spatial phase distribution in Fe, 2 wt-% Mn, 0.8 wt-% Cr after oxidation at $p(O_2)= 3 \cdot 10^{-22}$ bar and 700°C for 120min (left) and ternary phase diagram (right).

Mater. Sci. Forum **969** (2011) 76-81.

Segregation

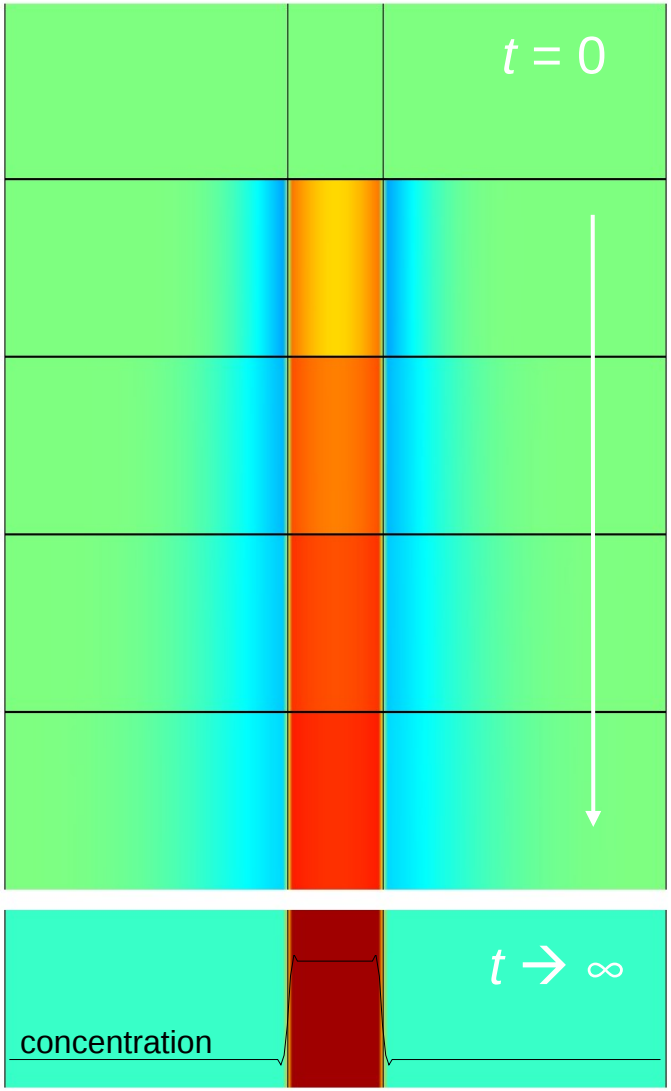

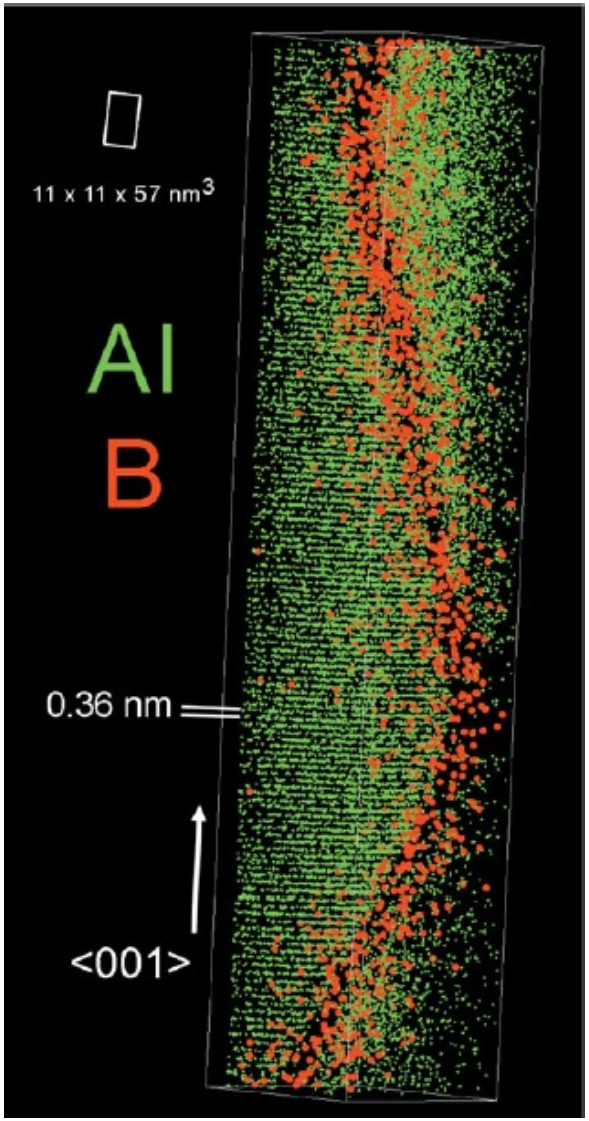

Figure: Numerical simulation of „uphill-diffusion“ (left) and 3D atom probe tompgraphy of segregated boron atoms in a NiAl grain boundary (right).

APT - Blavette et.al. *Microsc. Microanal.* **13** (2007) 464.

Thermodynamics in real life

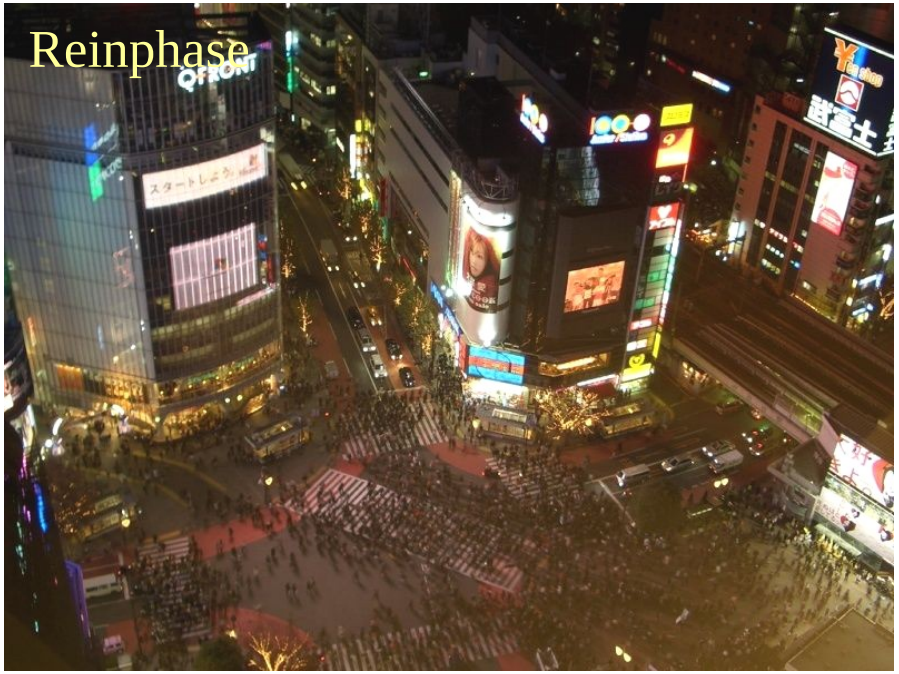

$$J_A = -D\,\nabla c \qquad\qquad J_A = -L\,\nabla \mu$$

$$J_A = -L\,\nabla\mu = -L\,\frac{\partial \mu}{\partial c}\nabla c = \cdots = \underbrace{-L\frac{RT}{c}}_{D}\nabla c - L\left(\nabla \mu^o + \frac{RT}{\gamma}\nabla\gamma\right)$$

Figure: Street cossing in Shibuya (渋谷 , Japan) at red and green traffic signal.

Oxide and Nitride Formation

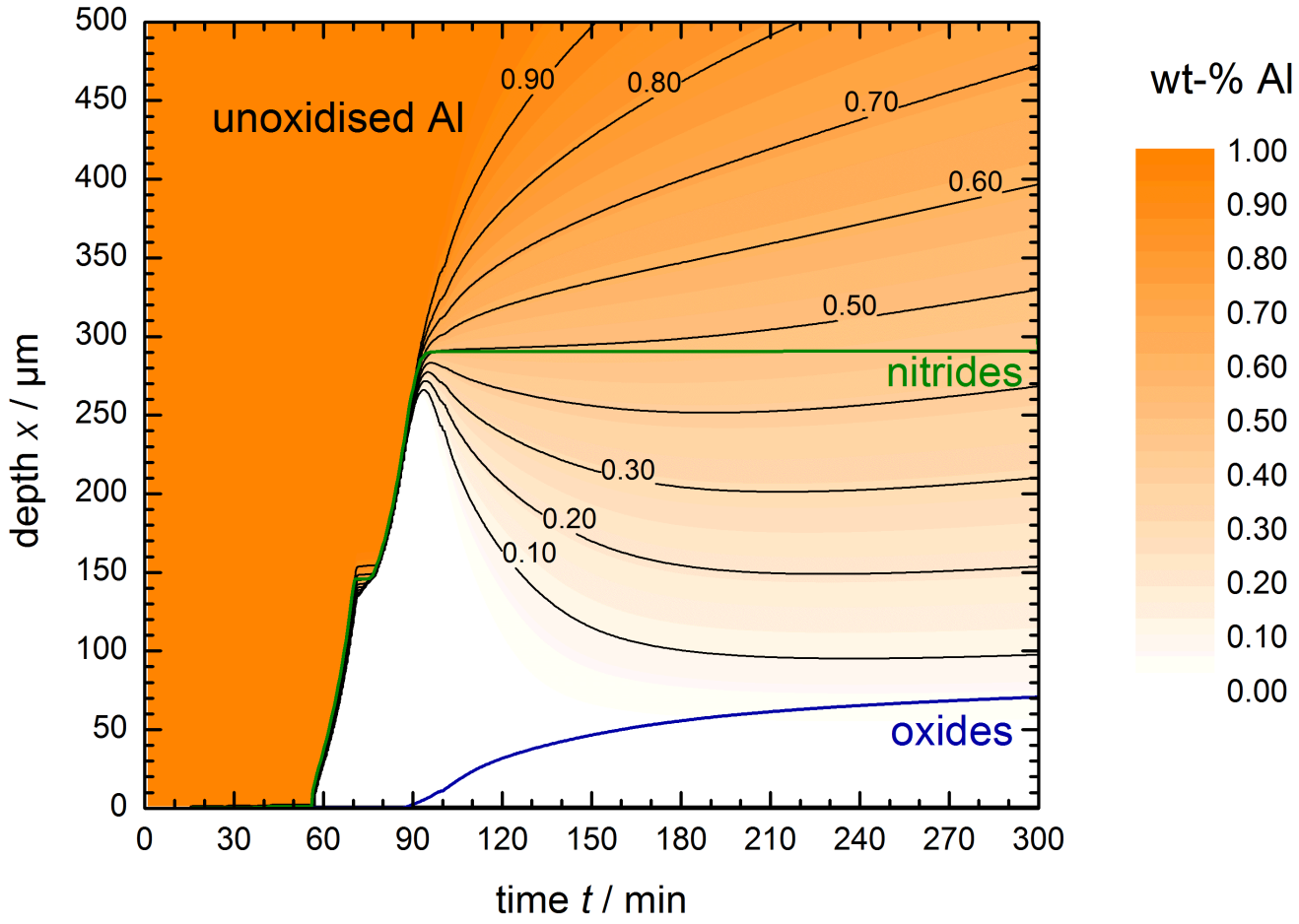

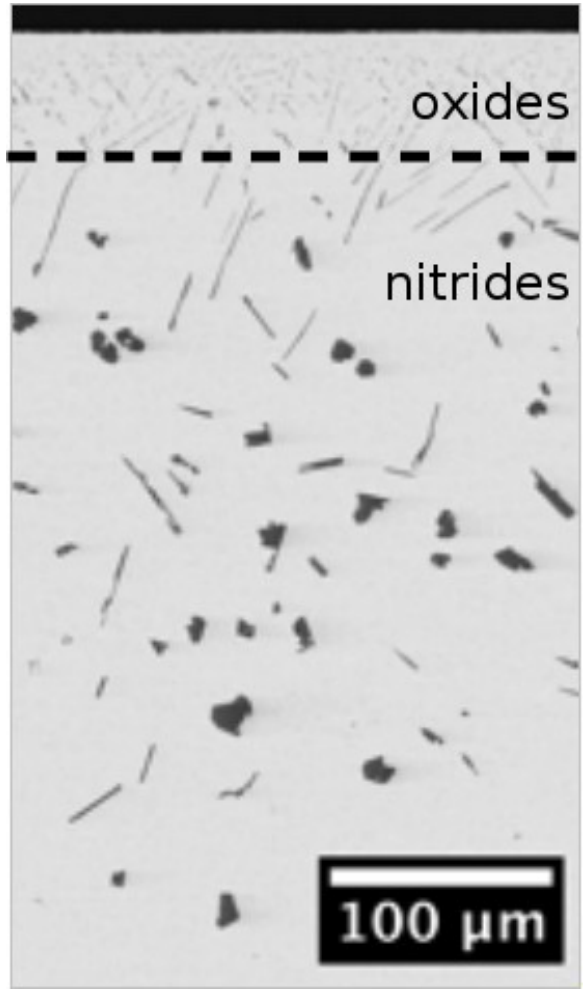

Figure: Calculated corrosion depth in Fe, 1wt-%Al, oxidised with N_2 / 2.5vol-% H_2 / 0.1vol.% H_2O (left) and SEM-picture of the cross section after 300min (right).

J.H. Bott et.al., submitted

Oxide and Nitride Formation

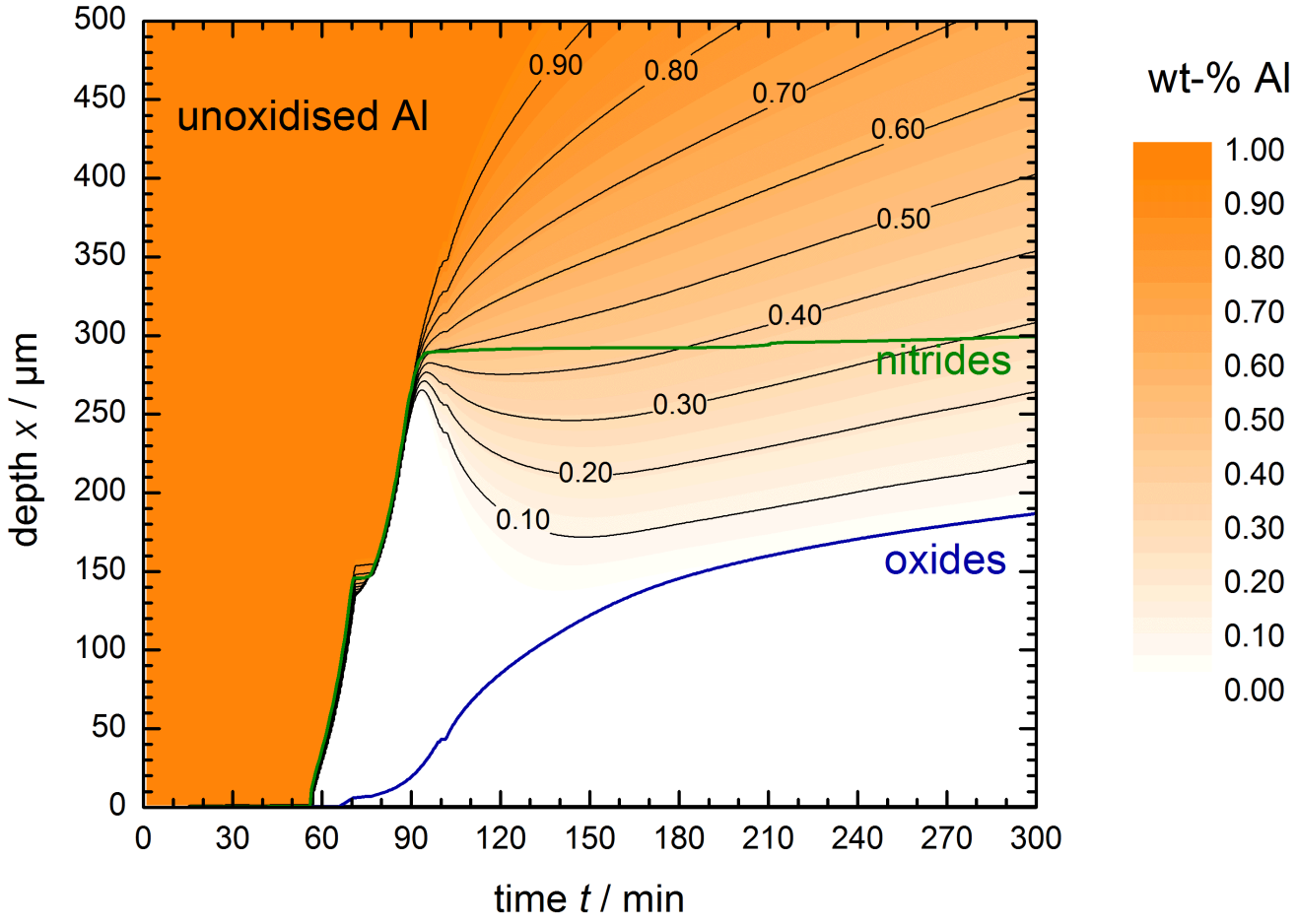

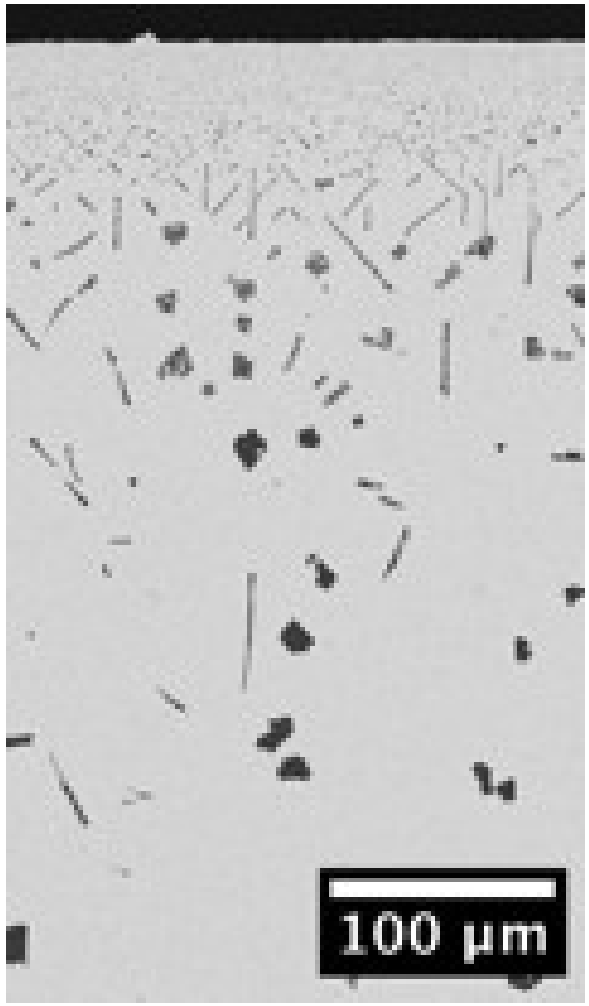

Figure: Calculated corrosion depth in Fe, 1wt-%Al, oxidised with N_2 / 2.5vol-% H_2 / 1.08vol.% H_2O (left) and SEM-picture of the cross section after 300min (right).

J.H. Bott et.al., submitted

Wagner's-Criterion for Internal Oxidation

internal oxidation ⟶ external oxidation

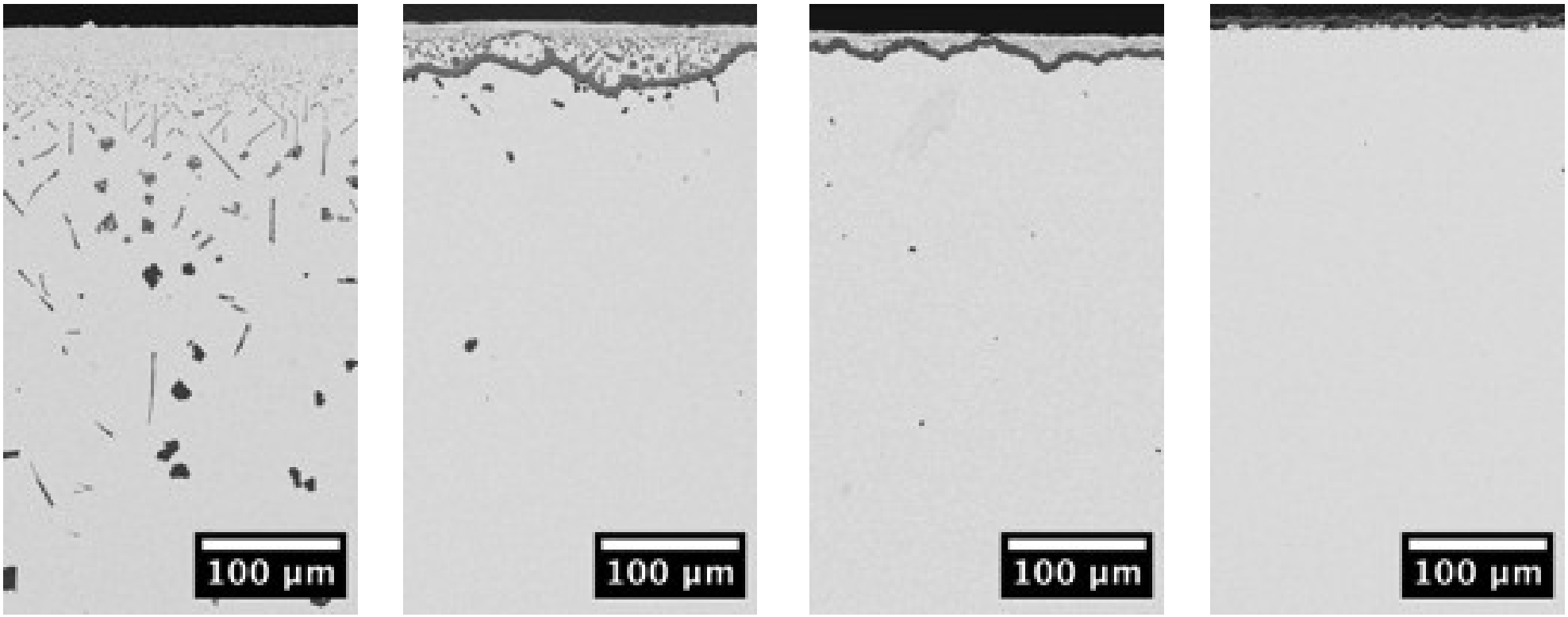

Fe, 1wt-% Al | Fe-3Al | Fe-5Al | Fe-8Al

Figure: SEM-pictures of cross sectioned Fe-Al alloys after exposure to temperatures ≤ 1285 °C in N_2 / 2.5 vol-% H_2 / 1.08vol.% H_2O (DP +8°C) atmosphere.

J.H. Bott et.al., submitted

Decarburizsation of Pearlite

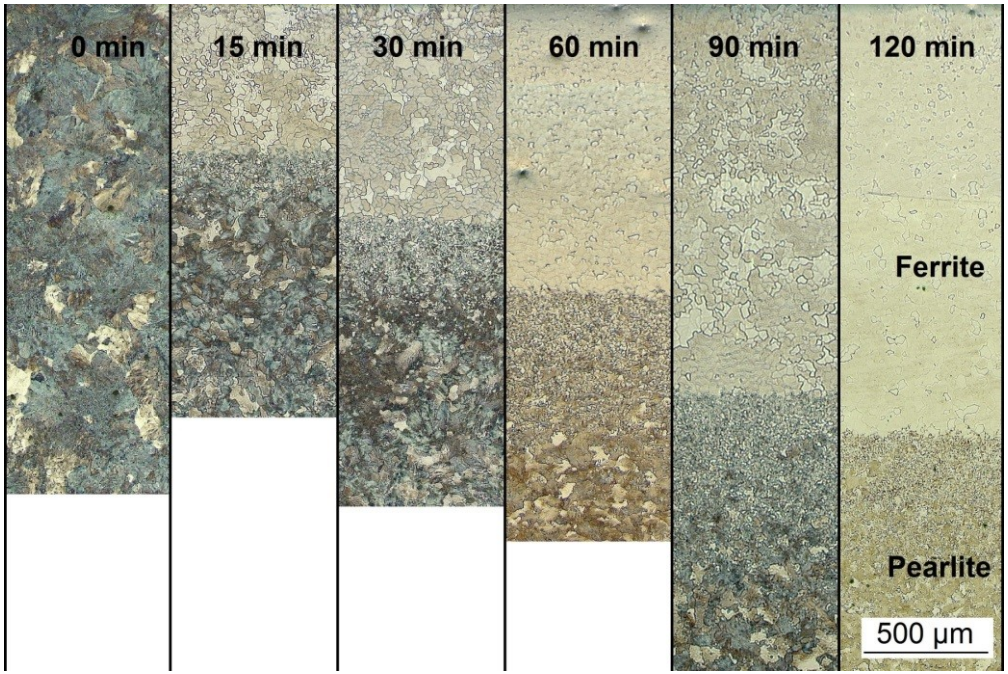

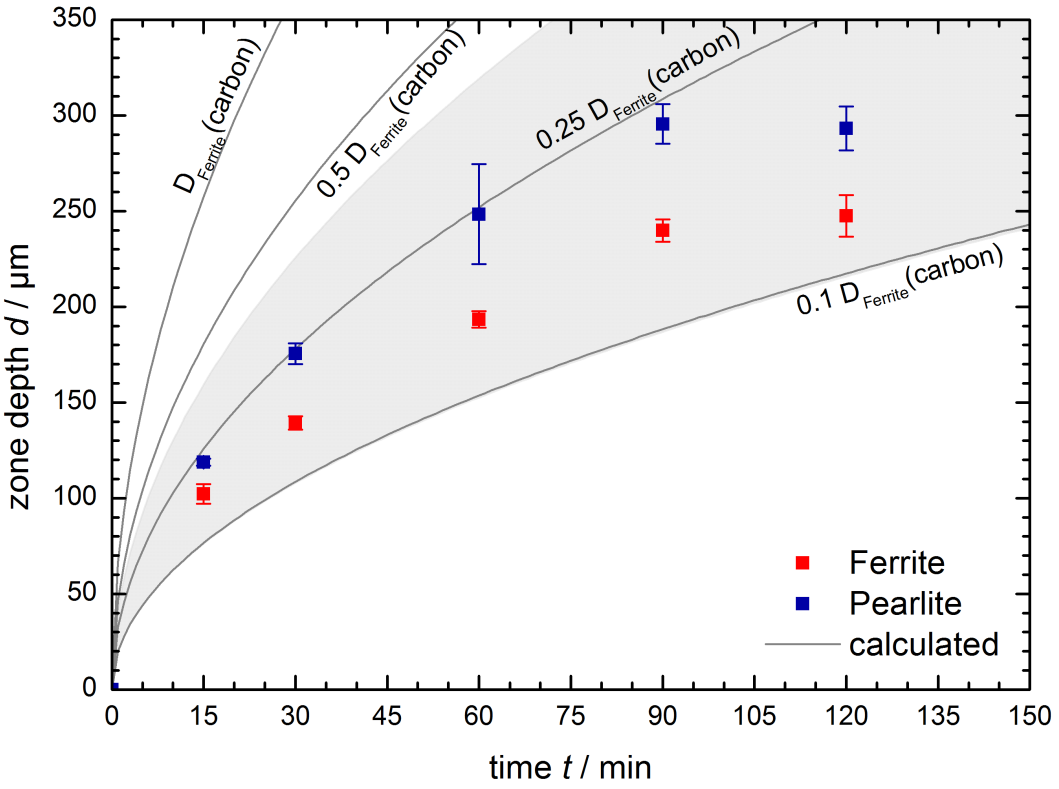

Figure: Angled cross section (7°) of Fe, 0.8 wt-% C after heat treatment at 800°C in Ar / 2.5 vol-% H_2 / 1.5 vol-% H_2O and etching with 1% Nital for 15s.

Corros. Sci. **78** (2014) 188-192.

Properties of Oxygen

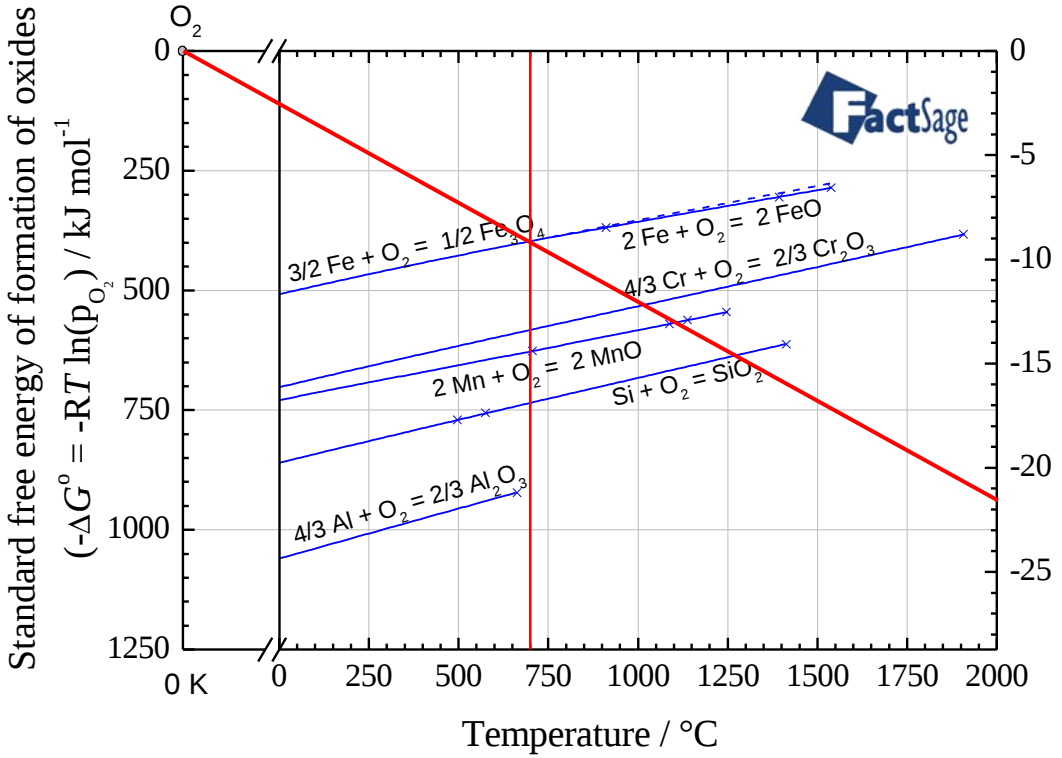

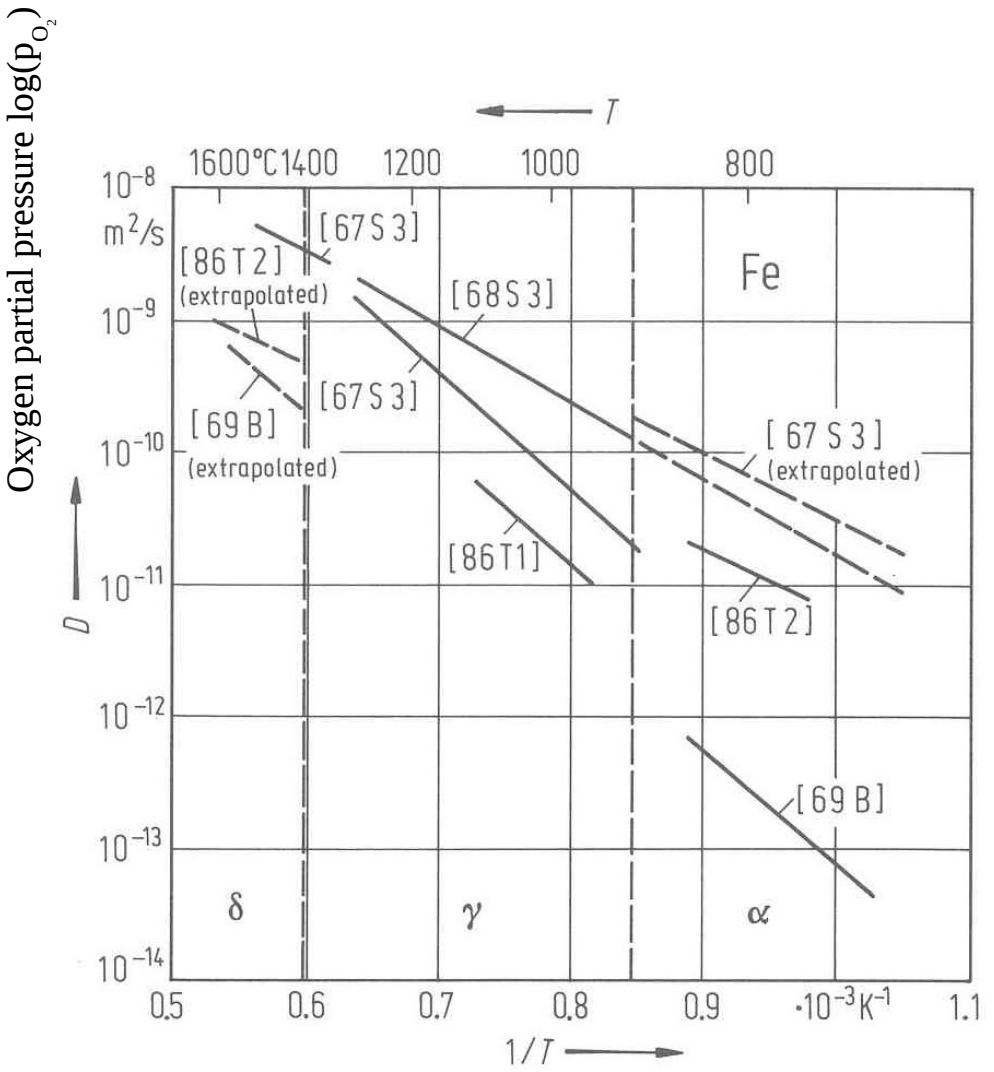

Fig. 23. Fe. Diffusion coefficient for O diffusion in α, γ and δ-phase Fe vs. (reciprocal) temperature.

Theoretical Background

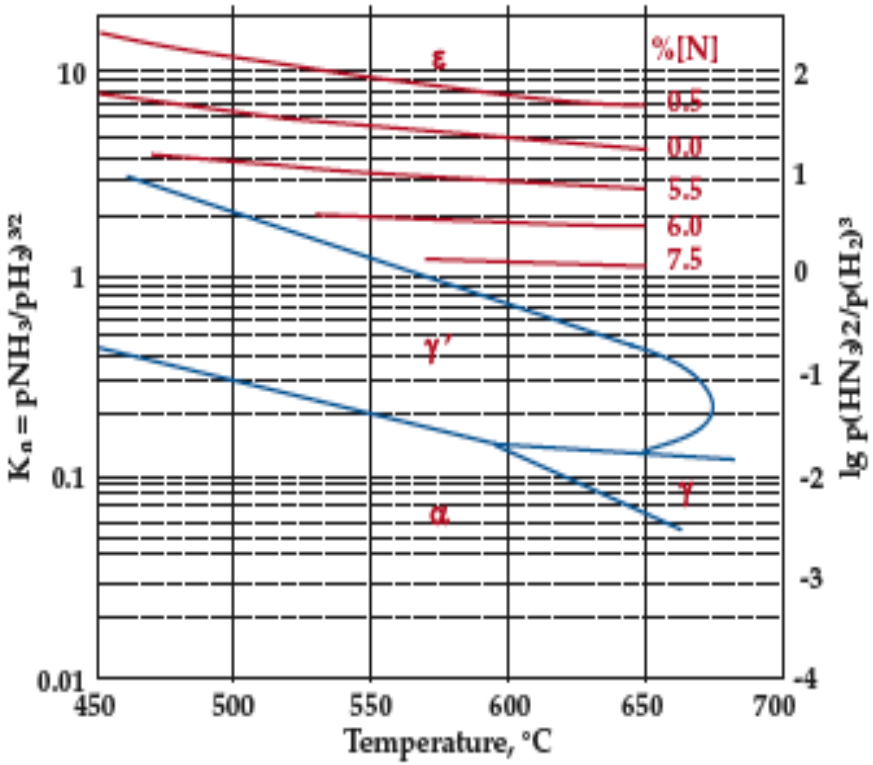

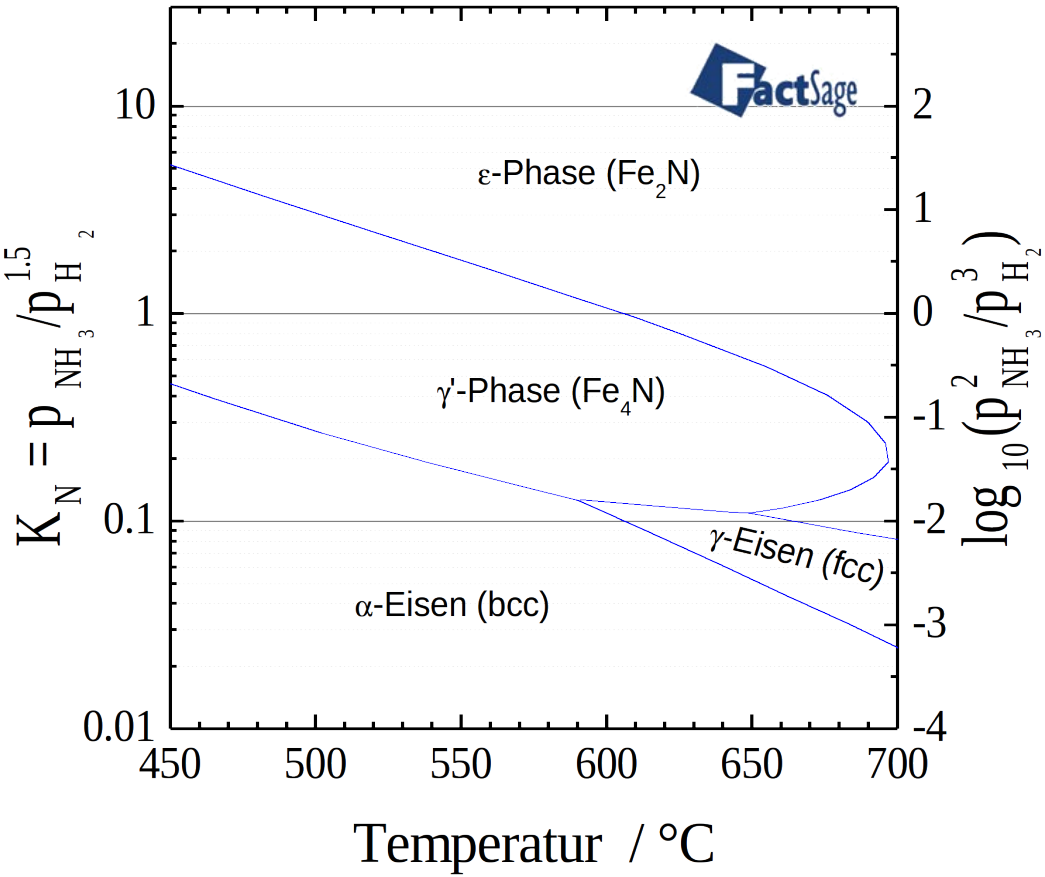

Figure: Lehrer diagram of iron nitride phases from literature (left) and calculated with FactSage (right).

www.ipsenusa.com (left diagram)

Iron-Chromium-Carbon Alloy

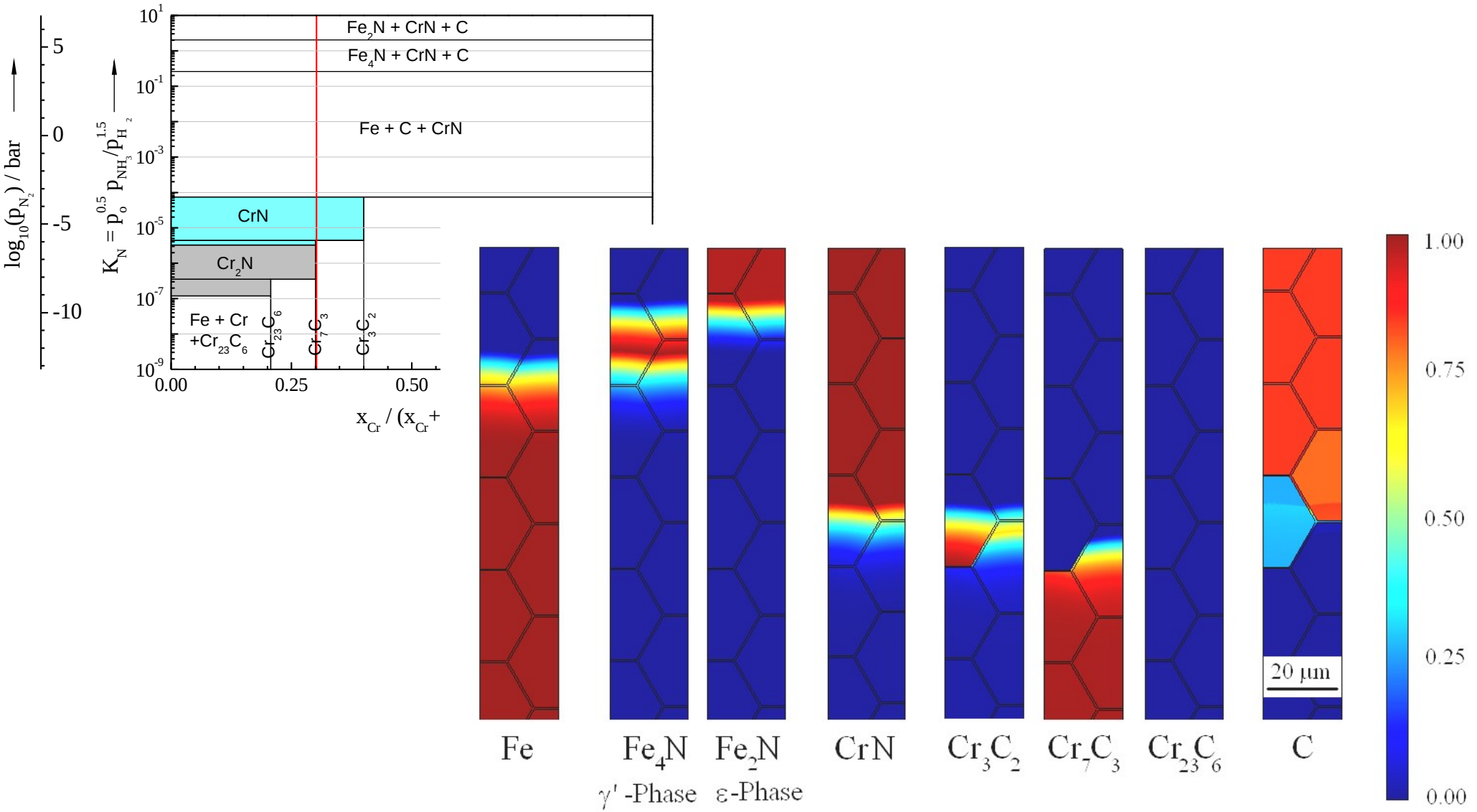

Figure: Spatial phase distribution in an Fe, 1 wt-% Cr, 0.1 wt-% C alloy after gas nitriding at K_N= 2.4 and 500 °C for 48 h and phase stability diagram.

HTM J. Heat Treatm. Mat. **66** (2011) 100-102.

Nitriding of AISI H11 (5%Cr, 0.35%C)

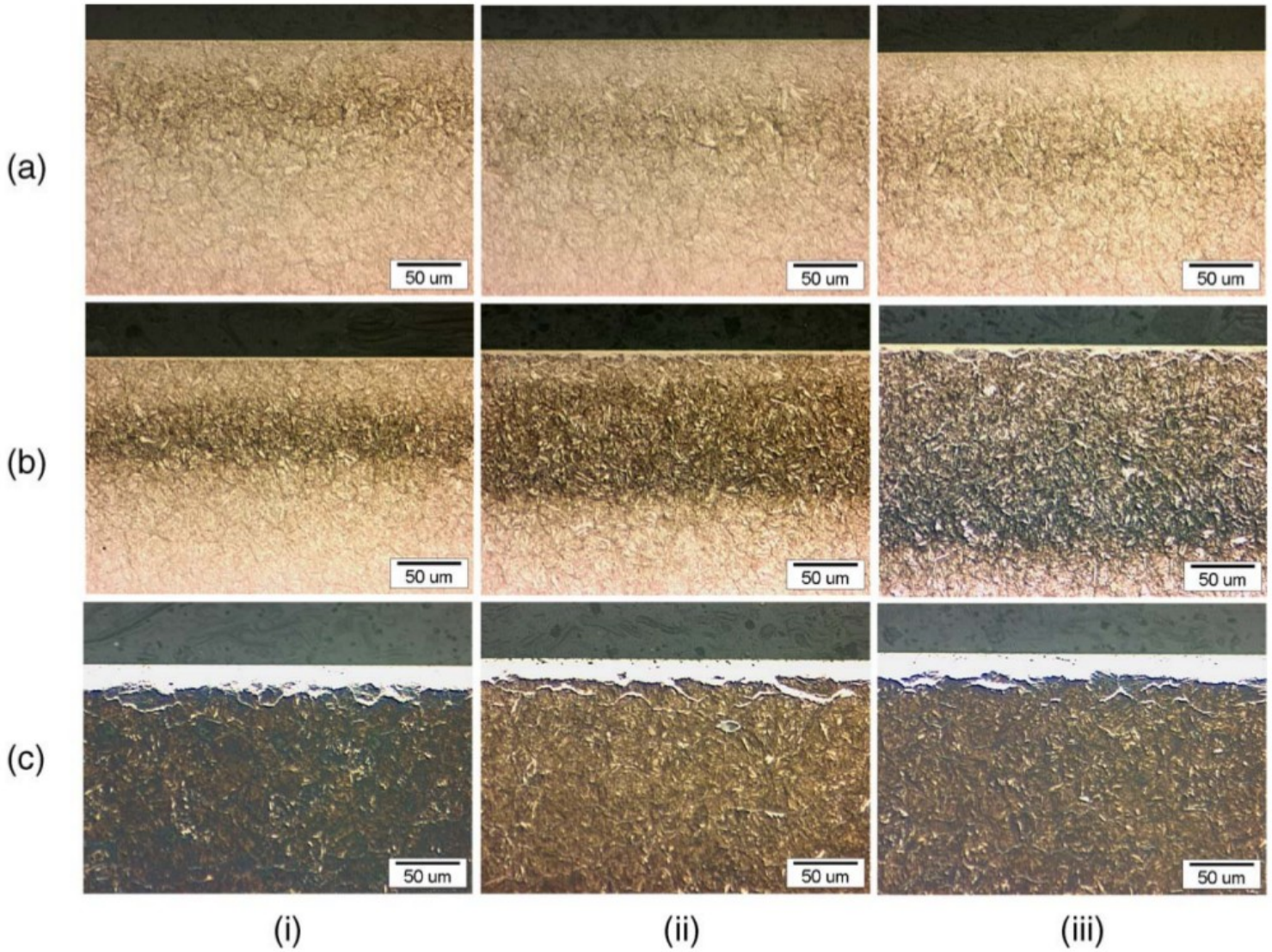

Fig. 4. Optical micrographs showing the cross-sectional microstructure for processing temperatures of (a) 480 °C, (b) 540 °C and (c) 580 °C. For each temperature, the processing times are (i) 8 h, (ii) 16 h and (iii) 32 h.

D. Nolan et.al. *Surf. Coat. Technol.* **201** (2006) 182.

Hydrogen in Steel

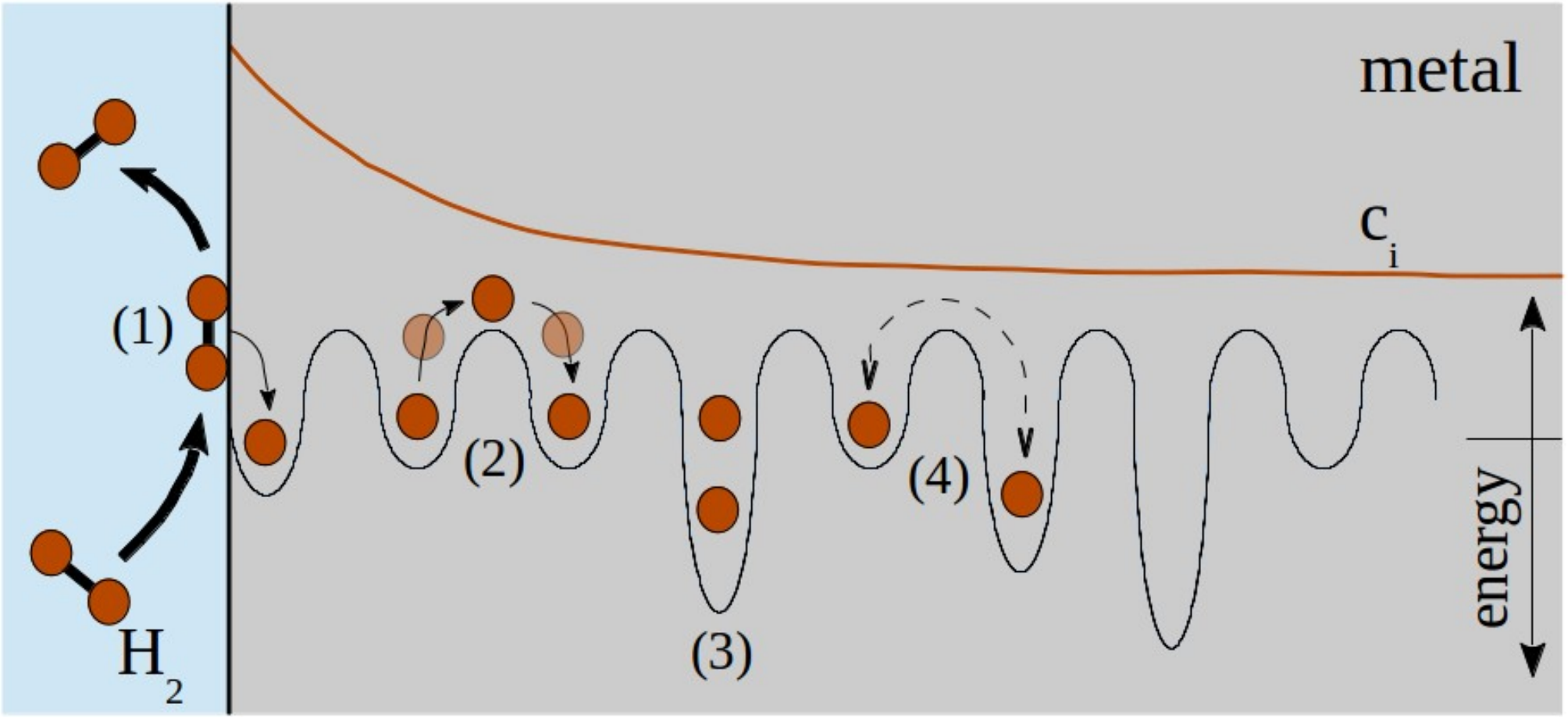

Figure: Ilustration of hydrogen transport in crystalline materials. Effects of surface (1), diffusion (2), solubility (3) and trapping (4).

Chem. Phys. Chem. (2014) *accepted*.

„Effective“ Diffusion

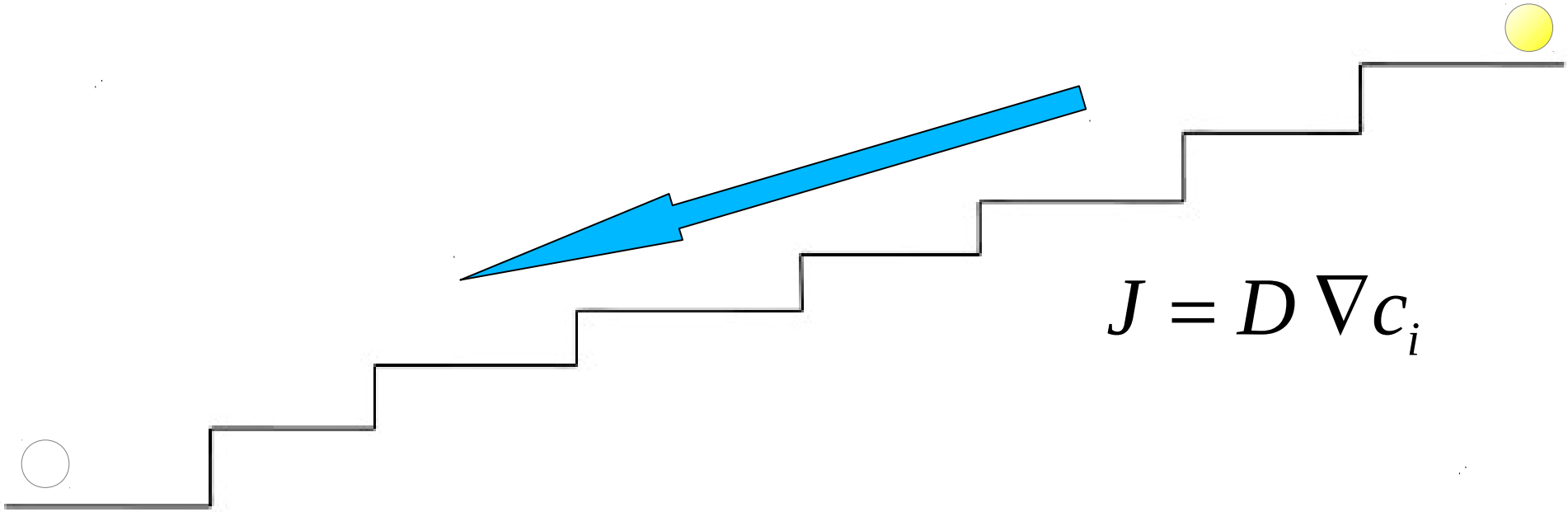

$$J = D \nabla c_i$$

„Effective“ Diffusion

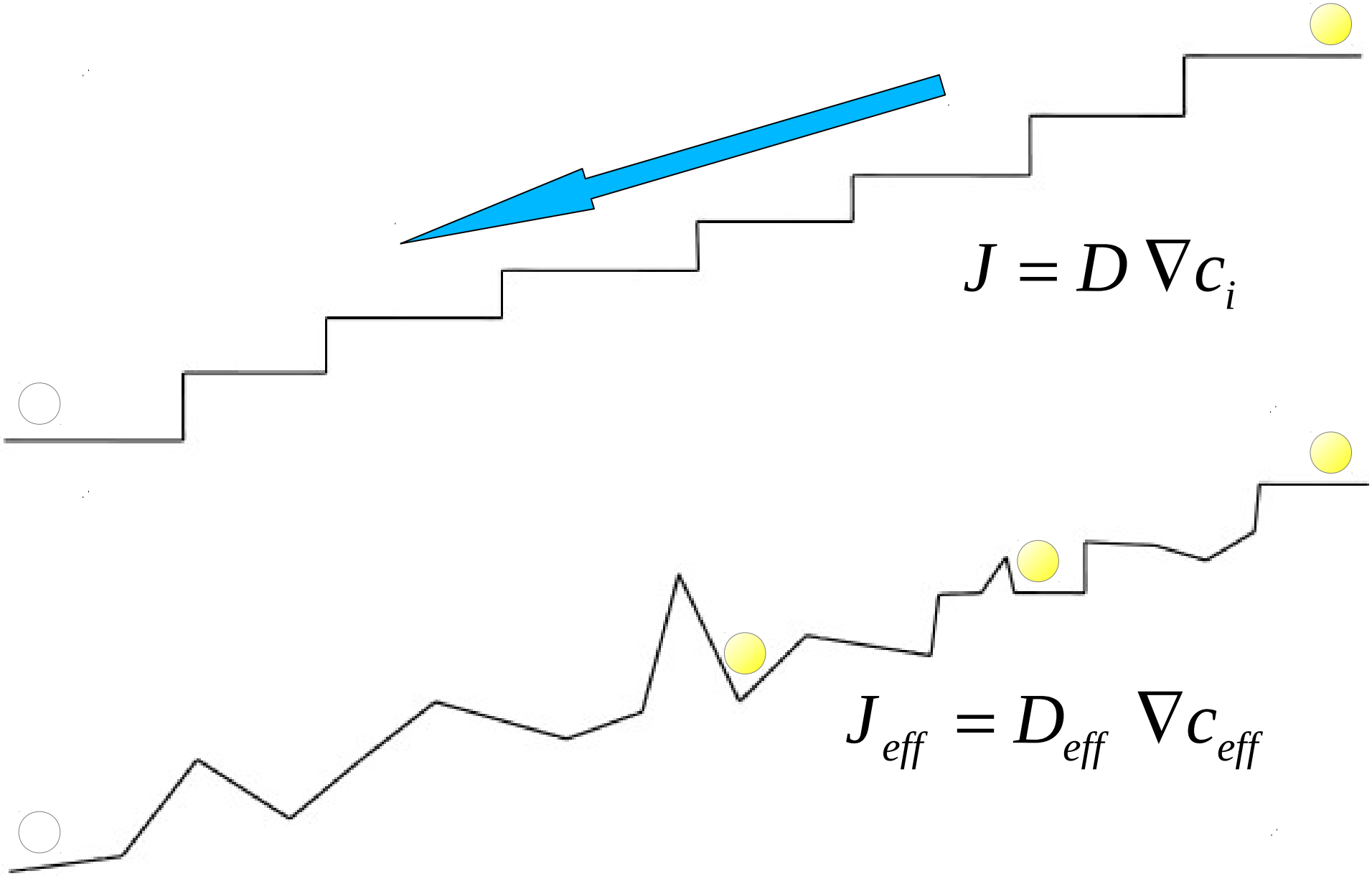

$$J = D \nabla c_i$$

$$J_{eff} = D_{eff} \nabla c_{eff}$$

Theoretical Background

$$H_i + \square_j \rightleftharpoons \square_i + H_j$$

$$c_j = c_j^{\max} \frac{c_i K_j}{c_i^{\max} + c_i\left(K_j - 1\right)}$$

$$c_{ges} = c_i + \sum_j c_j$$

$$\frac{\partial c_{ges}}{\partial t} = \frac{\partial}{\partial x}\left\{D \frac{\partial c_{ges}}{\partial x}\right\}$$

$$\left\{1 + \sum_j \frac{c_j^{\max} c_i^{\max} K_j}{\left[c_i^{\max} + c_i\left(K_j - 1\right)\right]^2}\right\} \frac{\partial c_i}{\partial t} = D \frac{\partial^2 c_i}{\partial x^2}$$

$$\frac{\partial c_i}{\partial t} = \underbrace{\frac{D}{\left\{1 + \sum_j \frac{c_j^{\max} c_i^{\max} K_j}{\left[c_i^{\max} + c_i\left(K_j - 1\right)\right]^2}\right\}}}_{D_{eff}} \frac{\partial^2 c_i}{\partial x^2}$$

$$K_{j\ (T)} = e^{\frac{Q_j}{RT}}$$

$$D_{(T)} = D^0\ e^{\frac{Q}{RT}}$$

Chem. Phys. Chem. (2014) *accepted*.

Desorption at Constant Heating Rate

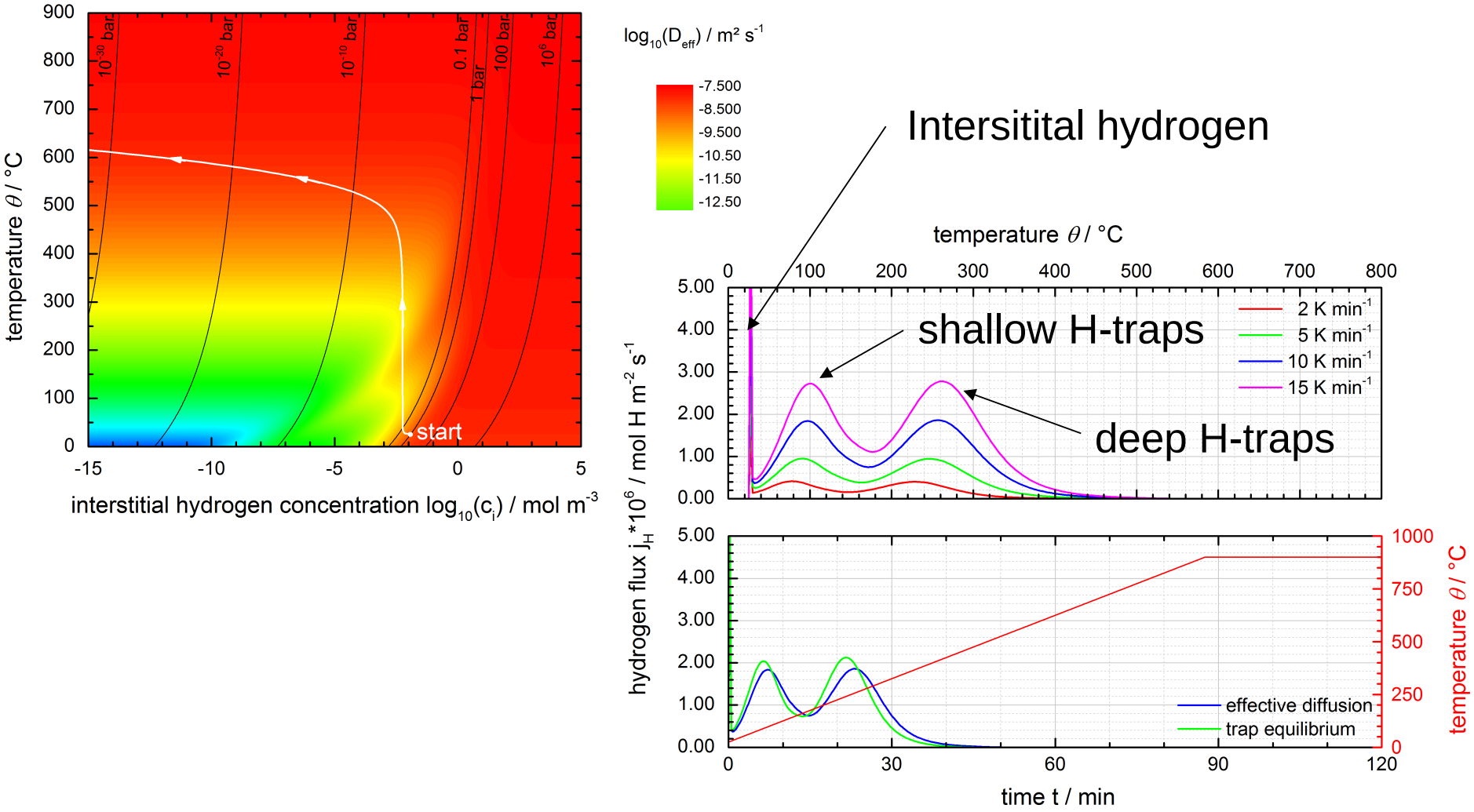

Figure: Effective diffusion coefficient in an idealized Fe-C alloy. Hydrogen traps are calculated as H_1 = -58.6 kJ (10 molH m^{-3}), H_2 = -84 kJ (15 molH m^{-3})

Chem. Phys. Chem. (2014) *accepted*.

Isothermal Hydrogen Diffusion

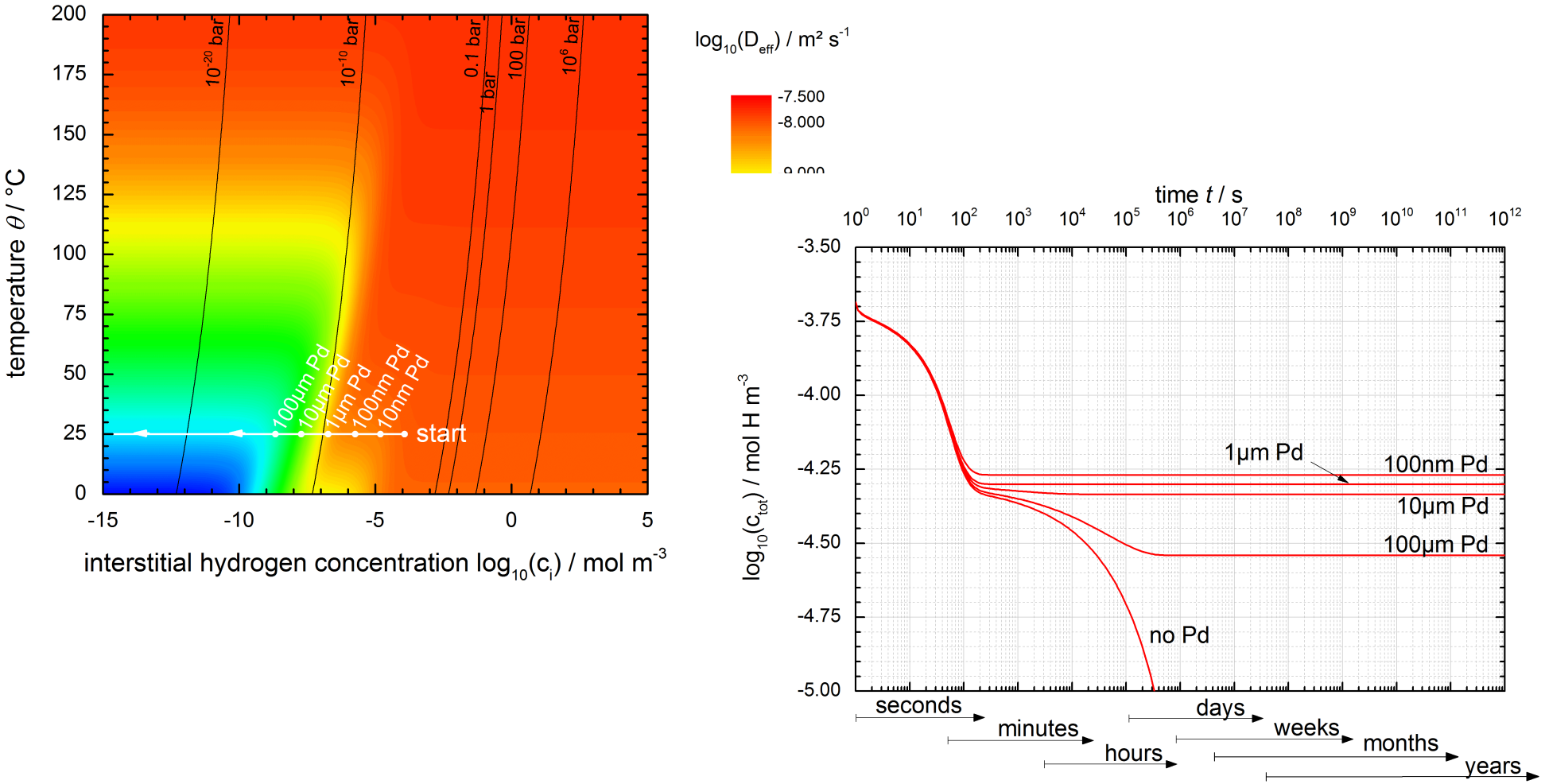

Figure: Effective diffusion coefficient in an idealized Fe-C alloy. Hydrogen traps are calculated as H_1 = -58.6 kJ (0.05 molH m^{-3}), H_2 = -84 kJ (0.05 molH m^{-3})

Chem. Phys. Chem. (2014) *accepted*.

Program Structure

element transport ⇄ chemical reaction

$$\frac{dc_{i(x,t)}}{dt} = \mathrm{div}\left(D_{i(x,T)}.\nabla c_{i(x,t)}\right)$$

CHEMAPP

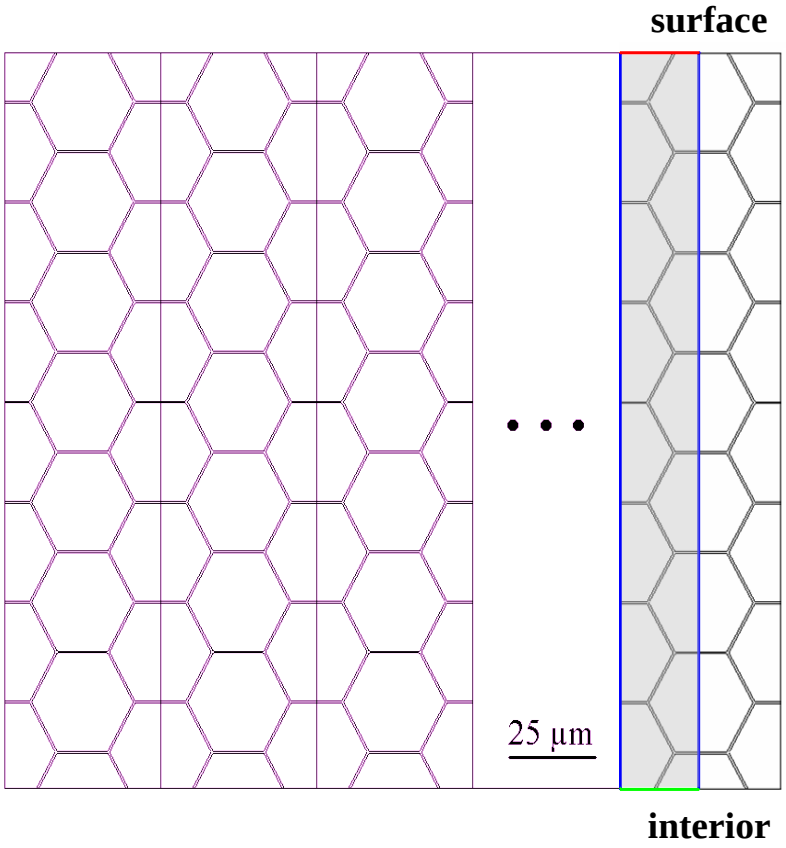

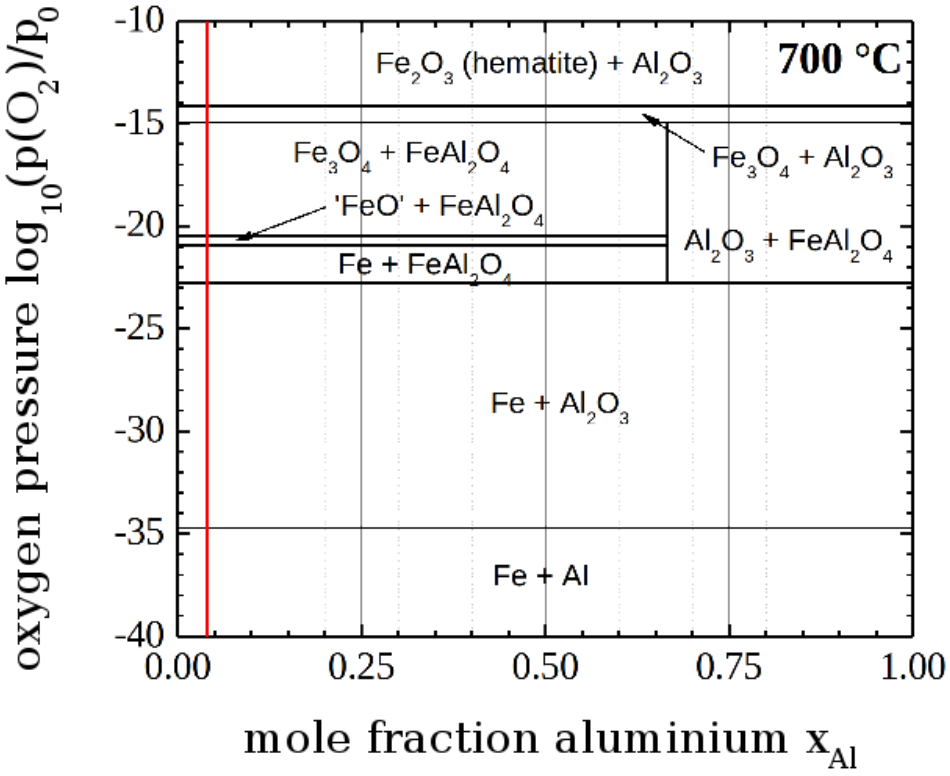

"ASTRID", Oxid. Met.. **76** (2011) 247-258.

Program Structure

element transport

chemical reaction

$$\frac{dc_{i(x,t)}}{dt} = \mathrm{div}\left(D_{i(x,T)}.\nabla c_{i(x,t)}\right)$$

CHEMAPP

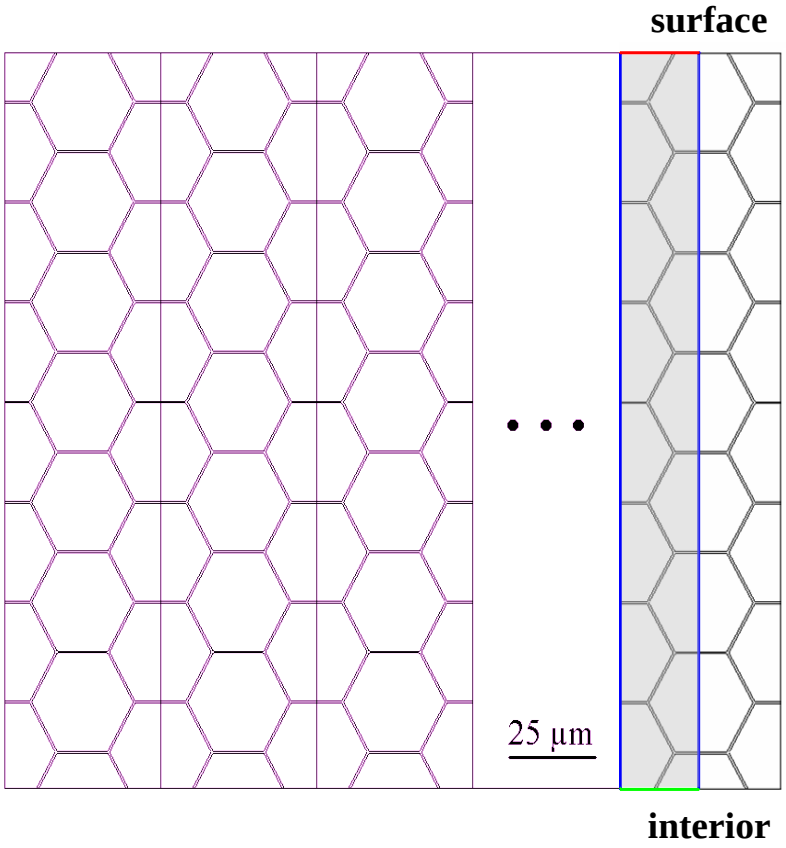

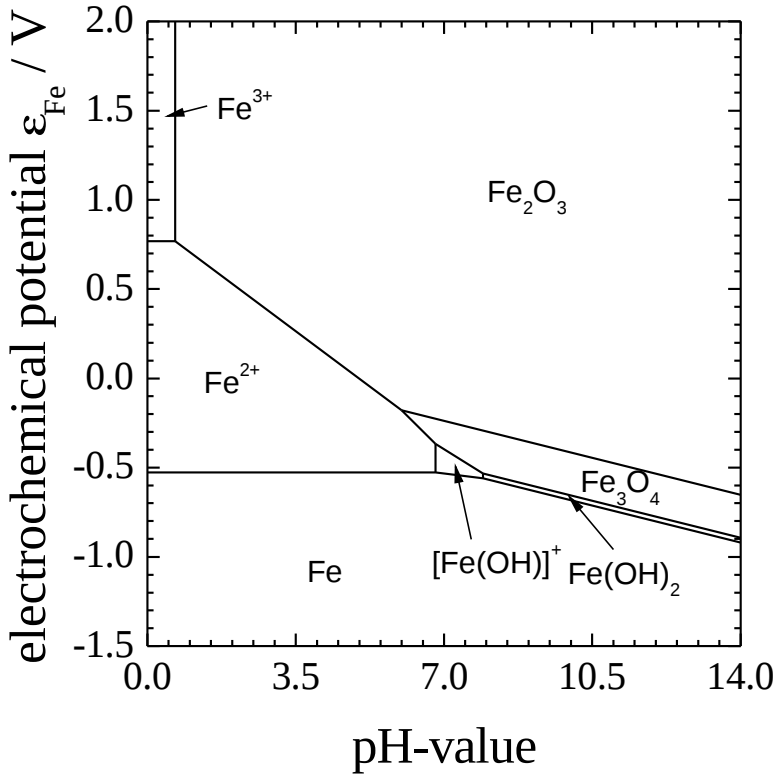

"ASTRID", *Oxid. Met.*. **76** (2011) 247-258.

Program Structure

element transport ⇄ chemical reaction

$$\frac{dc_{i(x,t)}}{dt} = \mathrm{div}\left(D_{i(x,T)}.\nabla c_{i(x,t)} + z_i.\mu_{i(x,T)}.c_{i(x,t)}.\nabla\phi_{(x,t)}\right)$$

CHEMAPP

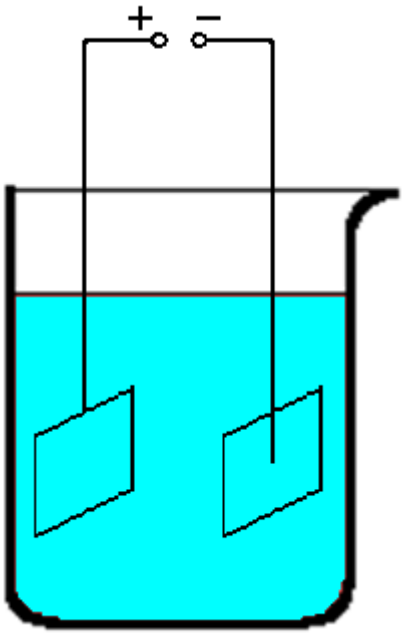

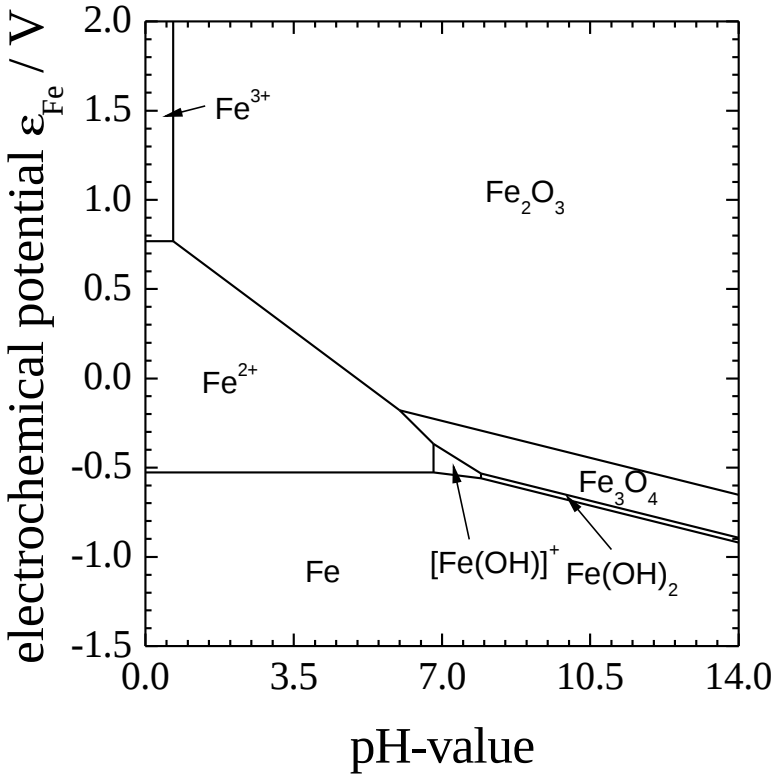

"ASTRID", Oxid. Met.. **76** (2011) 247-258.

Electrochemistry and Surface pH-values

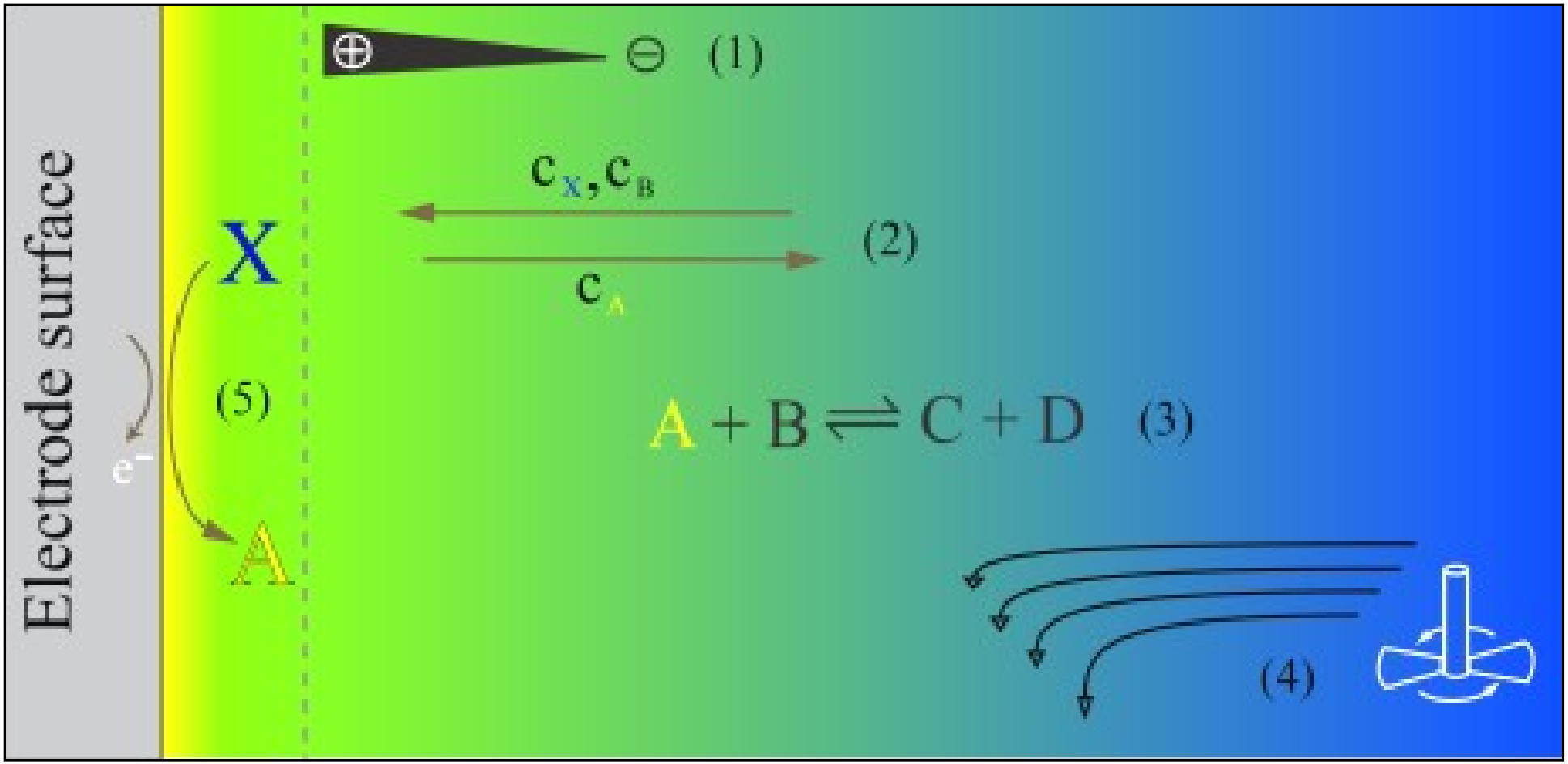

PCCP (2011) **13** 16384

Local Corrosion Effects

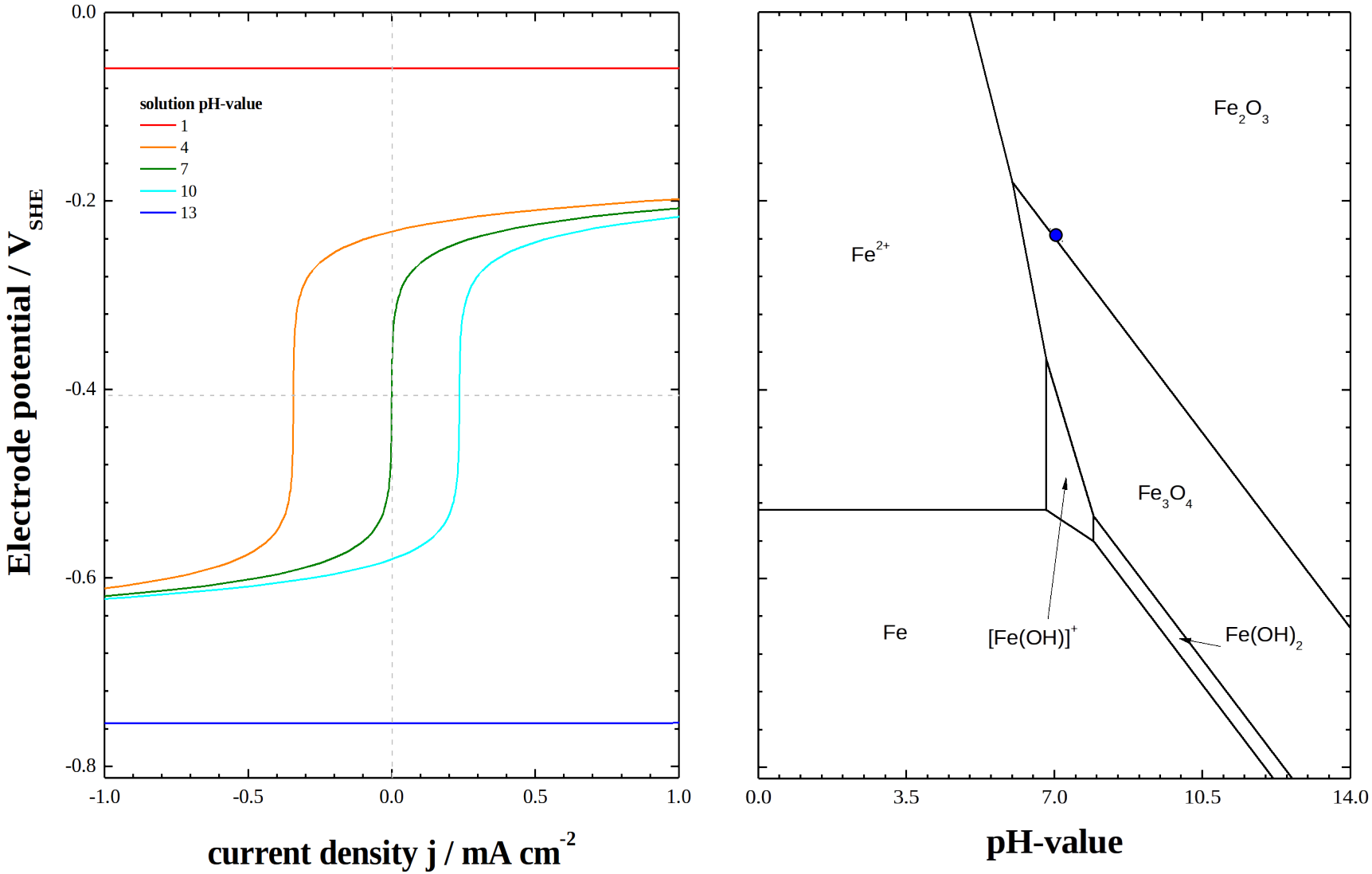

Figure: Cyclic voltammograms in unbuffered solutions of different pH-value.

Local Corrosion Effects

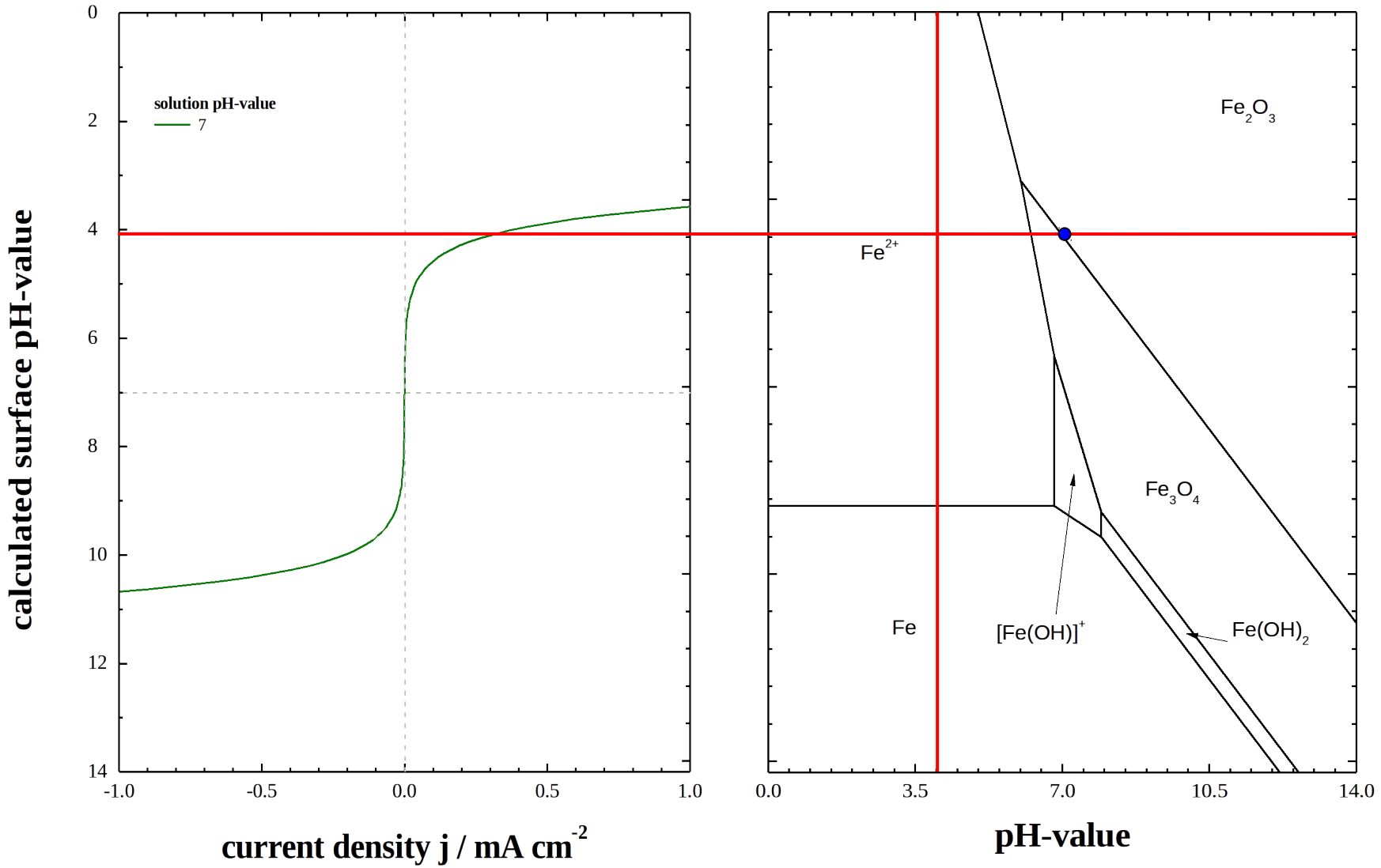

Figure: Cyclic voltammogram in unbuffered solution of pH 7.

General Transportation Scheme

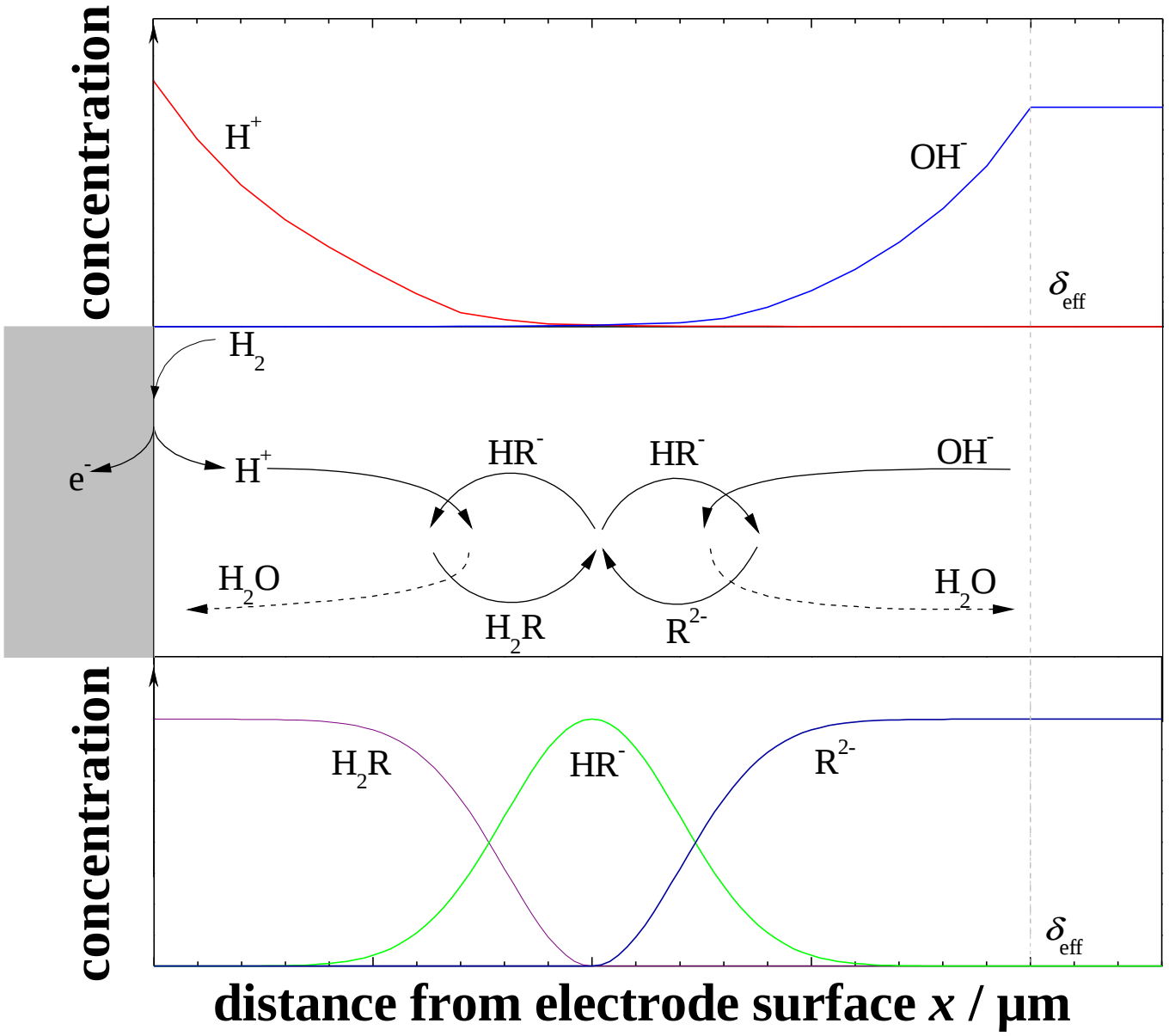

PCCP (2011) **13** 16384

Acetate Buffered Solution

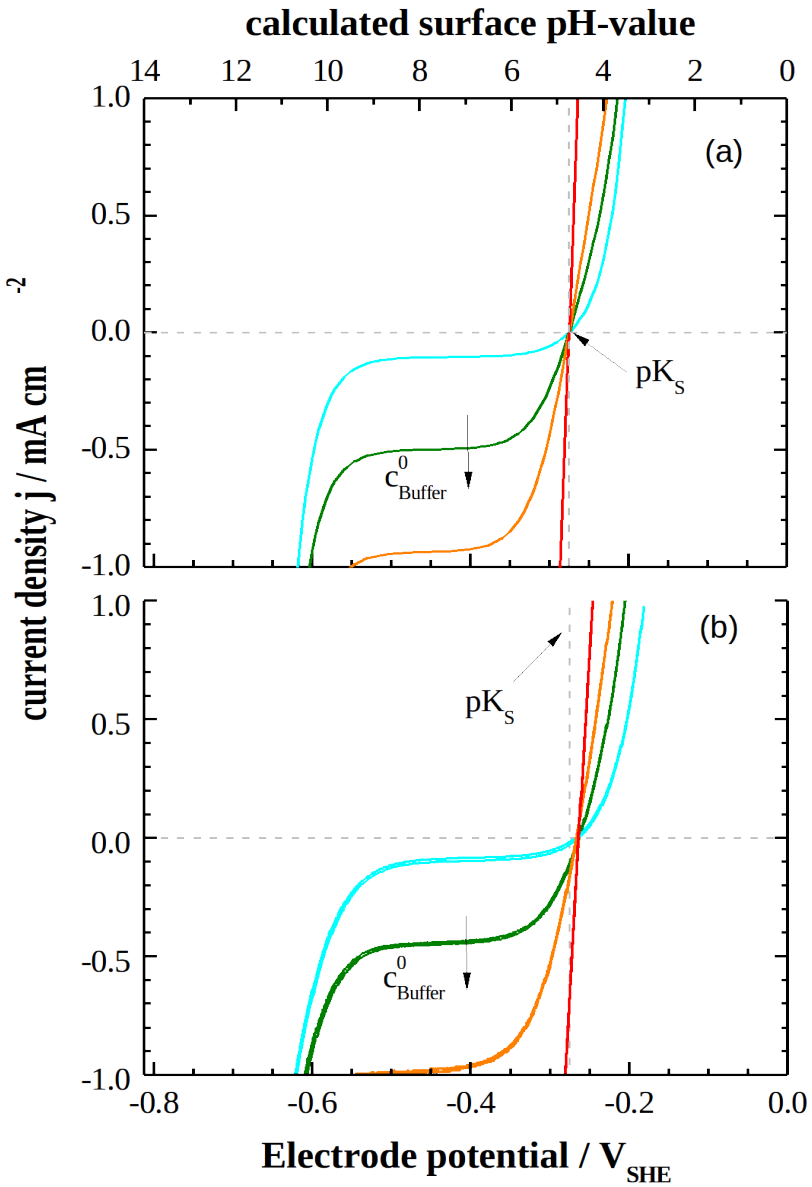

$$CH_3COOH \rightleftharpoons CH_3COO^- + H^+$$

PCCP (2011) **13** 16384

Acetate Buffered Solution

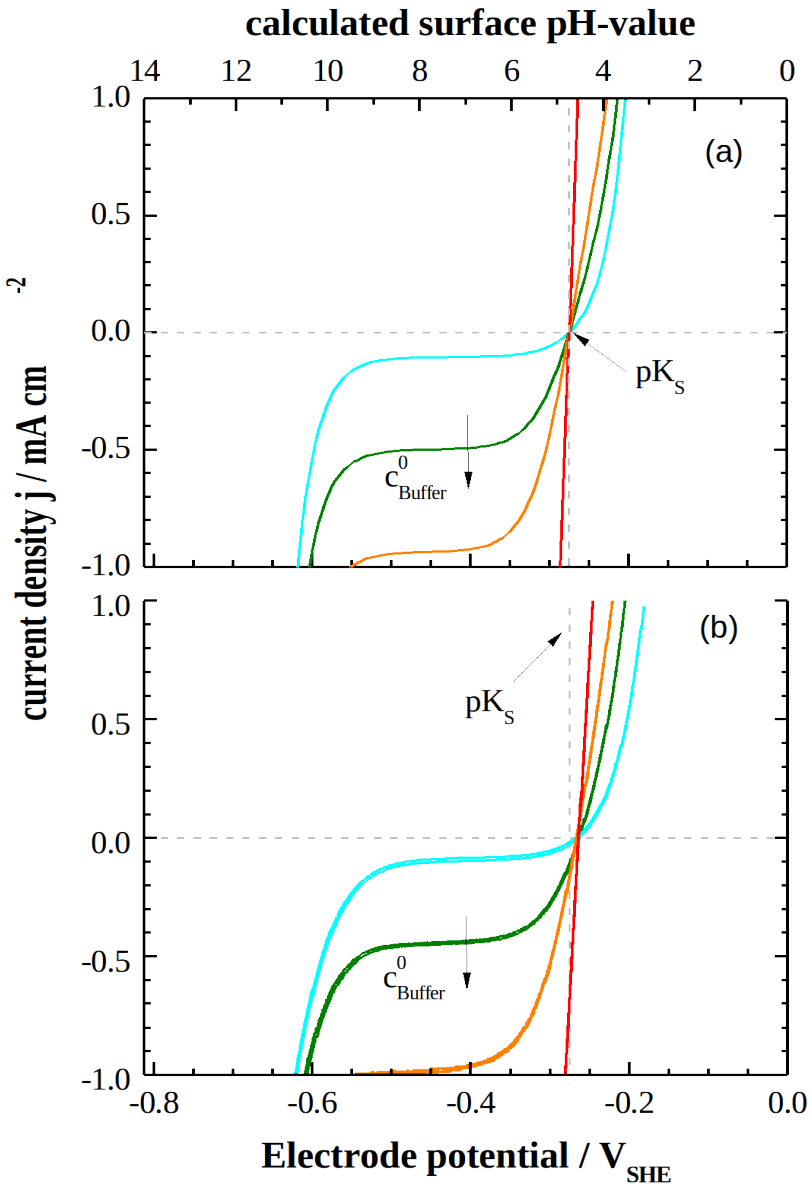

$$CH_3COOH \rightleftharpoons CH_3COO^- + H^+$$

$$j = j_{H^+/OH^-} + \frac{c^0_{Buffer}\,F}{\delta_{eff}}\left[\frac{D_{HAc}\,c_H^{surface} - D_{Ac^-}K_S}{K_S + c_H^{surface}} - \frac{D_{HAc}\,c_H^{solution} - D_{Ac^-}K_S}{K_S + c_H^{solution}}\right]$$

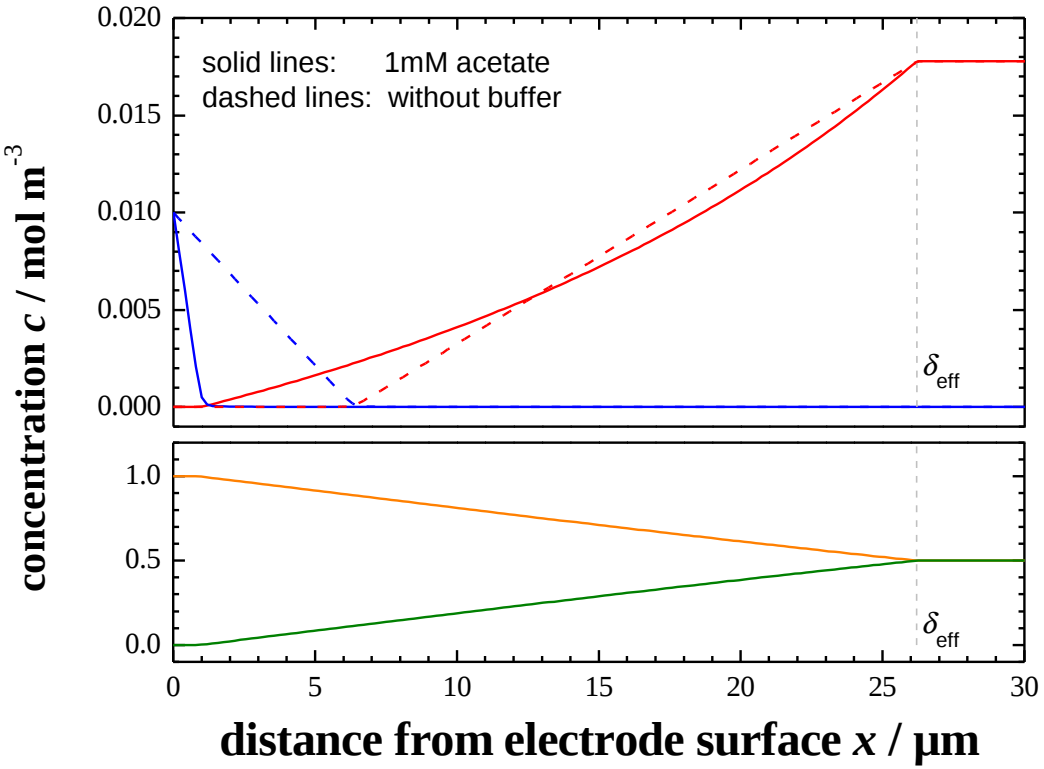

PCCP (2011) **13** 16384

Phosphate Buffered Solution

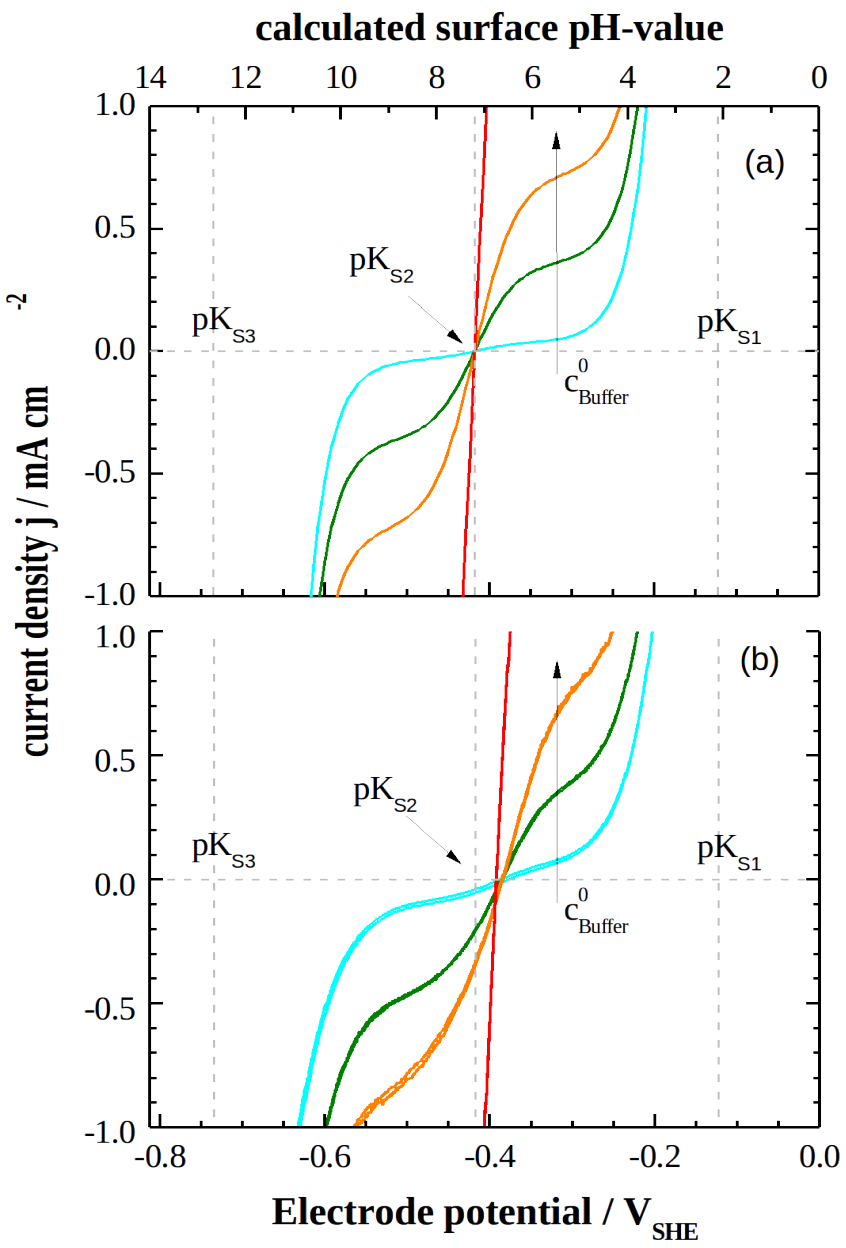

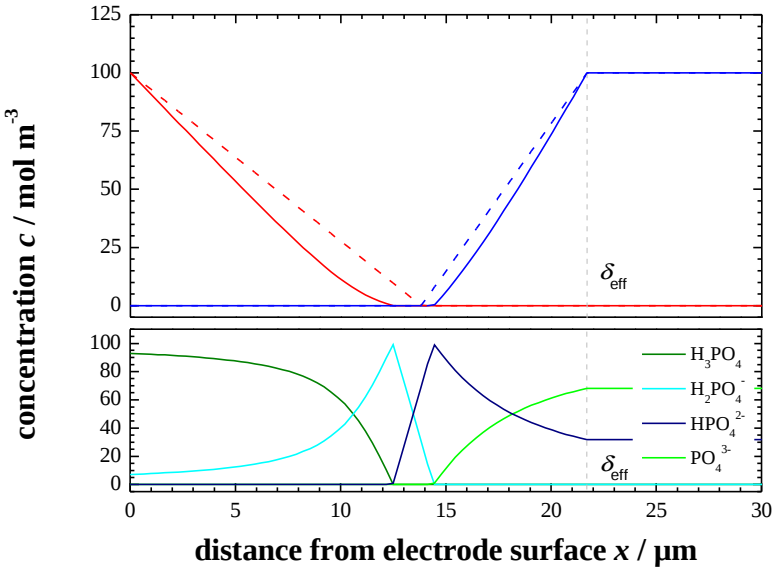

$$j = j_{H^+/OH^-} + j_{Buffer}$$

$$j_{Buffer} = \frac{c^0_{Buffer}\,F}{\delta_{eff}} \left(\frac{3D_1 + D_2 \frac{K_{S1}}{c_{(x),H^+}} - D_3 \frac{K_{S1}K_{S2}}{c^2_{(x),H^+}} - 3D_4 \frac{K_{S1}K_{S2}K_{S3}}{c^3_{(x),H^+}}}{1 + \frac{K_{S1}}{c_{(x),H^+}} + \frac{K_{S1}K_{S2}}{c^2_{(x),H^+}} + \frac{K_{S1}K_{S2}K_{S3}}{c^3_{(x),H^+}}} \right)_{x=\delta_{eff}}^{x=0}$$

Summary

Modelling High Temperature Oxidation in Iron-Chromium Systems
M. Auinger, R. Naraparaju, H.-J. Christ, M. Rohwerder
Oxid. Met. 76 (2011) 247-258

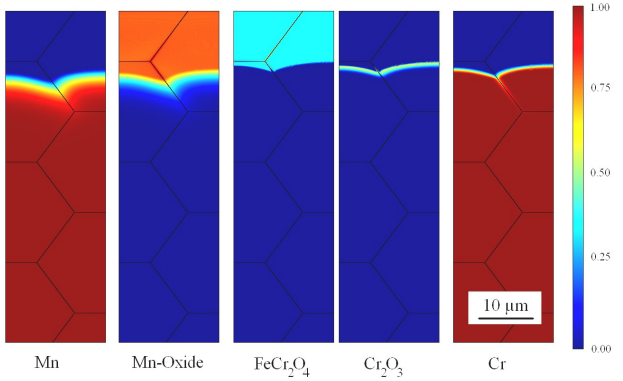

Thermodynamic Stability and Reaction Sequence for High Temperature Oxidation Processes in Steels
M. Auinger, S. Borodin, S. Swaminathan and M. Rohwerder
Mater. Sci. Forum. 696 (2011) 76-81

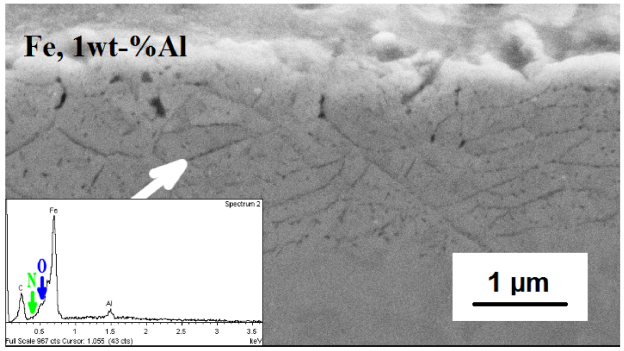

Modelling and Experiment of Selective Oxidation and Nitridation of Binary Model Alloys at 700°C - The Systems Fe, 1 wt-%{Al, Cr, Mn, Si}
M. Auinger, E.-M. Müller-Lorenz, M. Rohwerder, *Corros. Sci. accepted*

Thermogravimetry and in-situ mass spectrometry at high temperatures compared to theoretical modelling – The weight loss during selective decarburisation at 800 °C
M. Auinger, A. Vogel, V. G. Praig, H. Danninger, M. Rohwerder
Corros. Sci. 78 (2014) 188-192

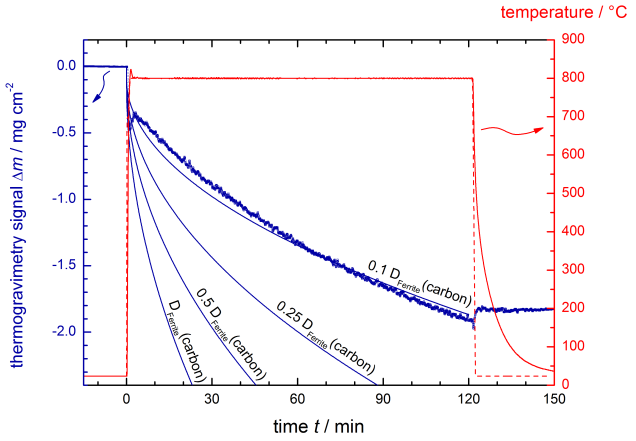

Summary

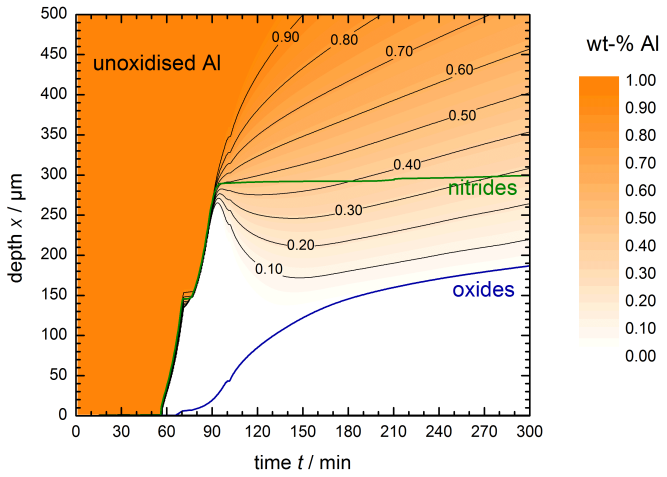

Selective Precipitation of Oxides and Nitrides in Fe-Al Alloys
J.H. Bott, H. Yin, S. Sridhar, M. Auinger
submitted

Hydrogen Transport in non-ideal Crystalline Materials
M. Auinger, *Chem. Phys. Chem. (2014)*
DOI:10.1002/cphc.201402001

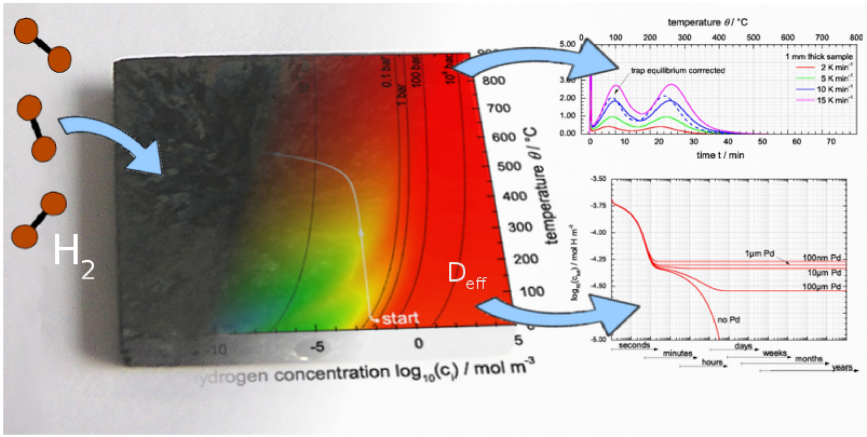

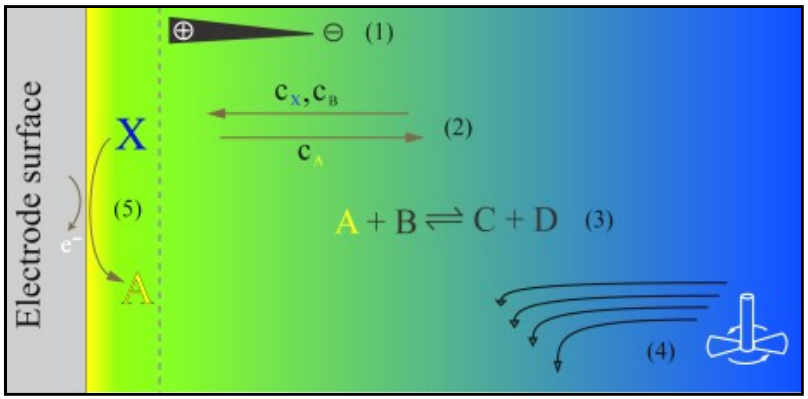

Near-surface ion distribution and buffer effects during electrochemical reaction
M. Auinger, I. Katsounaros, J.C. Meier, S.O. Klemm, P.U. Biedermann, A.A. Topalov, M. Rohwerder, K.J.J. Mayrhofer
Phys. Chem. Chem. Phys. 13 (2011) 16384-16394

Financial Support

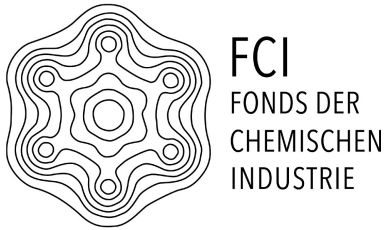

Acknowledgements

Max-Planck-Institut
für Eisenforschung GmbH

K. Mayrhofer, M. Rohwerder, J. Meier, M. Nellessen,

D. Kurz, I. Katsounaros, A. Mingers

Prof. Danninger

V. Praig

Prof. Seetharaman (now Uni Warwick)

J. Bott, J. Zhu

Dr. Paesold

B. Linder, K. Rendl, A. Muhr